RESEARCH REPORT

EJN European Journal of Neuroscience   FENS   WILEY

Ageing-related changes in nap neuroscillatory activity are mediated and moderated by grey matter volume

Ahren B. Fitzroy[1,2] | **Kyle A. Kainec[1,2]** | **Rebecca M. C. Spencer[1,2,3]**

[1]Neuroscience and Behavior Program, University of Massachusetts Amherst, Amherst, MA, USA

[2]Department of Psychological and Brain Sciences, University of Massachusetts Amherst, Amherst, MA, USA

[3]Institute for Applied Life Sciences, University of Massachusetts Amherst, Amherst, MA, USA

Correspondence
Rebecca M. C. Spencer, Institute for Applied Life Sciences, Life Science Laboratories S315, 240 Thatcher Road, Amherst, MA 01003 USA.
Email: rspencer@umass.edu

Abstract

Ageing-related changes in grey matter result in changes in the intensity and topography of sleep neural activity. However, it is unclear whether these findings can be explained by ageing-related differences in sleep pressure or circadian influence. The current study used high-density electroencephalography to assess how grey matter volume differences between young and older adults mediate and moderate neuroscillatory activity differences during a midday nap following a motor sequencing task. Delta, theta, and sigma amplitude were reduced in older relative to young adults, especially over frontocentral scalp, leading to increases in relative delta frontality and relative sigma lateral centroposteriority. Delta reductions in older adults were mediated by grey matter loss in frontal medial cortex, primary motor cortex, thalamus, caudate, putamen, and pallidum, and were moderated by putamen grey matter volume. Theta reductions were mediated by grey matter loss in primary motor cortex, thalamus, and caudate, and were moderated by putamen and pallidum grey matter volume. Sigma changes were moderated by putamen and pallidum grey matter volume. Moderation results suggested that across frequencies, young adults with more grey matter had increased activity, whereas older adults with more grey matter had unchanged or decreased activity. These results provide a critical extension of previous findings from overnight sleep in a midday nap, indicating that they are not driven by sleep pressure or circadian confounds. Moreover, these results suggest brain regions associated with motor sequence learning contribute to sleep neural activity following a motor sequencing task.

Abbreviations: ACME, average causal mediation effect; ADE, average direct effect; BDI, Beck Depression Inventory; EEG, electroencephalogram; EMG, electromyogram; EOG, electrooculogram; EMM, estimated marginal mean; ESS, Epworth Sleepiness Scale; eTIV, estimated total intracranial volume; FIR, finite impulse response; FSL, FMRIB Software Library; GMV, grey matter volume; HD-PSG, high-density polysomnography; IIR, infinite impulse response; MEQ, Morningness-Eveningness Questionnaire; MMSE, Mini-Mental State Exam; MPRAGE, magnetisation-prepared rapid gradient echo; MRI, magnetic resonance imaging; NREM, non-rapid eye movement; NREM2, non-rapid eye movement stage 2; NREM3, non-rapid eye movement stage 3; OA, older adults; PSQI, Pittsburg Sleep Quality Index; REM, rapid eye movement; ROI, region of interest; SRTT, serial reaction time task; SSS, Stanford Sleepiness Scale; TICS, Telephone Interview for Cognitive Status; TST, total sleep time; VBM, voxel-based morphometry; YA, young adults.

1 | INTRODUCTION

Sleep is not unitary. Rather, sleep is composed of multiple stages: in humans, rapid eye movement (REM) and three stages of non-REM sleep are present, with each sleep stage serving a distinct array of cognitive and physiological functions (Iber, 2007; Rasch & Born, 2013). These stages are categorically classified by unique neural activity. REM is characterised by high-frequency electroencephalogram (EEG) activity resembling that of wake. Non-REM stage 2 (NREM2) is predominantly characterised by sleep spindles, discrete bursts of EEG activity in the sigma range (11–16 Hz), and K-complexes, discrete bursts of EEG activity in the middelta range (~2 Hz). Non-REM stage 3 (NREM3), also known as slow wave sleep, is characterised by large EEG oscillations in the delta (0.5–4 Hz) and theta (4–8 Hz) ranges (Dijk et al., 1990; Iber, 2007).

Neural activity during sleep can vary regionally. At the extreme, distinct sleep stages or even simultaneous sleep and wake are observed across different brain regions, a phenomenon known as local sleep (Huber et al., 2004; Nobili et al., 2012; Siclari & Tononi, 2017). More commonly, the intensity of neural activity within sleep-characteristic frequency bands varies regionally across a single sleep stage. Regional variation in sleep neural activity is prominent for the delta frequency band associated with slow wave sleep (Bersagliere et al., 2018; Nir et al., 2011; Nobili et al., 2011) and has also been reported for theta and sigma activity (Alfonsi et al., 2019; Andrillon et al., 2011; Nir et al., 2011; Nishida & Walker, 2007; Vyazovskiy & Tobler, 2005). To the extent that sleep neural activity varies regionally, ageing-related atrophy across different brain regions will have differential contributions to changes in sleep neural activity. The goal of the present study is to describe how reduced grey matter volume (GMV) across brain regions in older adults contributes to ageing-related changes in scalp-recorded neural activity during a midday nap.

1.1 | Changes in sleep EEG amplitude and topography across the lifespan

The regional variation of neural activity during sleep is reflected in topographic variations in scalp-recorded EEG, especially along the anterior–posterior axis (Finelli et al., 2001; Werth et al., 1997). In healthy young adults during overnight non-REM sleep, delta and theta are typically maximal over frontal scalp, whereas sigma is typically maximal over frontocentral scalp (Feinberg et al., 2011; Finelli et al., 2001; Werth et al., 1997). However, the topographic distribution of sleep EEG activity changes across the lifespan in a frequency band-specific manner (Feinberg et al., 2011; Kurth et al., 2010; Sprecher et al., 2016).

Developmentally, delta shifts from a primarily occipital distribution in early childhood to a primarily frontal distribution by early adolescence (Kurth et al., 2010). With typical ageing, sleep delta activity is reduced across the entire scalp (Carrier et al., 2001, 2011; Dijk et al., 1989; Gaudreau et al., 2001; Landolt et al., 1996; Landolt & Borbély, 2001; Schwarz et al., 2017; Sprecher et al., 2016), with larger reductions observed over frontal regions (Carrier et al., 2011; Münch et al., 2004; Robillard et al., 2010; Sprecher et al., 2016).

Theta during non-REM sleep also declines across the lifespan, but in a manner distinct from that observed for delta (Buchmann et al., 2011; Campbell & Feinberg, 2009; Feinberg et al., 2011; Kurth et al., 2010; Sprecher et al., 2016). Longitudinal work demonstrates that non-REM theta declines steadily from 9 to 11 years of age, while delta is unchanged across this interval (Campbell & Feinberg, 2009), and the clear developmental increase in the relative frontality of delta is largely absent for theta (Feinberg et al., 2011; Kurth et al., 2010). During typical ageing, non-REM theta continues to decline through middle and older adulthood (Carrier et al., 2001; Dijk et al., 1989; Gaudreau et al., 2001; Landolt et al., 1996), especially over frontocentral scalp regions (Landolt & Borbély, 2001; Sprecher et al., 2016).

Sigma activity decreases across infancy until around 2 years of age (Scholle et al., 2007; Tanguay et al., 1975), increases during early childhood (Kurth et al., 2010; McClain et al., 2016; Scholle et al., 2007), then decreases again through adolescence and early adulthood (Buchmann et al., 2011; Gaudreau et al., 2001; Kurth et al., 2010; Shinomiya et al., 1999). Like theta, sigma does not undergo a developmental shift in relative frontality and instead stays maximal over frontocentral scalp (Kurth et al., 2010). Sigma continues to decline through middle and older adulthood (Crowley et al., 2002; Dijk et al., 1989; Gaudreau et al., 2001; Nicolas et al., 2001; Peters et al., 2014; Schwarz et al., 2017), especially over frontocentral scalp regions (Landolt & Borbély, 2001; Mander et al., 2014; Martin

et al., 2013; Sprecher et al., 2016), leading to an ageing-related increase in the relative concentration of sigma over lateral centroposterior scalp regions (Sprecher et al., 2016).

1.2 | Relationships between sleep EEG and GMV across the lifespan

Changes in cortical grey matter across the lifespan follow a similar trajectory as that observed for delta. Peak GMV and thickness are reached in occipital cortex by 8 years of age, but frontal regions do not reach peak GMV or thickness until 13 years (Giedd et al., 1999; Gogtay et al., 2004; Shaw et al., 2008), which corresponds with increasing delta frontality across childhood. During adolescence, frontal and parietal cortical thinning correlates with and partially mediates maturational declines in frontocentral delta (Buchmann et al., 2011; Goldstone et al., 2018). In young adulthood, frontal delta amplitude is correlated with GMV in medial prefrontal cortical regions (Saletin et al., 2013). Later in life, ageing-related reductions in frontal delta are mediated by atrophy in medial frontal cortex and other frontal cortical regions (Dubé et al., 2015; Latreille et al., 2019; Mander et al., 2013). These parallel spatial changes in delta activity and grey matter over the lifespan have been interpreted as evidence that delta reflects frontal cortical maturation during development (Buchmann et al., 2011; Kurth et al., 2010) and may serve as a biomarker of and therapeutic target for frontal cortical atrophy during typical ageing (Mander et al., 2013).

Campbell and Feinberg (2009) posited that while developmental changes in delta reflect changes in frontal cortex and other neocortical structures, changes in non-REM theta may reflect development of allocortical structures such as the hippocampus. However, Buchmann et al. (2011) reported significant colocalisation of maturational correlations with non-REM theta power and cortical thickness in several neocortical regions during adolescence, but no such relationship between non-REM theta and grey matter in the (periallocortical) parahippocampal gyrus. Additionally, across a cohort of young and older adults Latreille et al. (2019) found an inverse relationship between spectrally relative non-REM theta and occipital cortical thickness but no relationship between spectrally relative non-REM theta and hippocampal volume. However, the spectral normalisation of theta amplitude to the broadband EEG employed by Latreille et al. (2019) caused their theta measure to be dependent on delta amplitude, potentially obscuring theta-specific relationships with allocortical grey matter. Characterising the extent to which reduced spectrally

isolated theta in older adults is mediated by atrophy in neocortical and allocortical structures would therefore help clarify the neural generators of theta across both maturation and ageing.

Sigma activity is also related to grey matter in an age-dependent manner (Fogel et al., 2017; Saletin et al., 2013). However, the brain regions in which grey matter influences sigma differ from those shown to influence delta. In young adults, Saletin et al. (2013) found that GMV in the hippocampus was related to a dominance of fast spindle activity, whereas GMV in insular and auditory cortices was related to a dominance of slow spindle activity. Fogel et al. (2017) also reported a relationship between spindle activity and GMV in the hippocampus, as well as in cingulate and parietal cortices, supplementary motor area, and cerebellum; these additional brain regions likely reflect performance of a motor sequencing task prior to sleep. The relationships between spindle measures and GMV reported by Fogel et al. (2017) were moderated by age, such that GMV correlated with spindle measures in young adults but not in older adults. The age moderation of the relationship between GMV and spindles following a motor sequence learning task is particularly interesting given prior evidence that ageing-related deficits in sleep-dependent memory consolidation are evident for motor sequence learning, but not declarative learning (Aly & Moscovitch, 2010; Fogel et al., 2014; Sonni & Spencer, 2015; Spencer et al., 2007; Terpening et al., 2013; Wilson et al., 2012). Following this, in the present study, we sought to determine whether age also moderated the relationships between GMV and sleep delta or theta activity following a motor sequencing task.

1.3 | Using naps to disentangle sleep from sleep pressure and circadian timing

The majority of previous investigations of ageing-related changes in the topography of sleep neural activity and its relationship to GMV have focused on overnight sleep, and those that have investigated naps have limited sleep physiology analysis to sleep spindles (Fogel et al., 2017). However, other aspects of sleep neural activity, particularly delta and theta, are known to be influenced by homeostatic sleep pressure (Münch et al., 2004; Robillard et al., 2010). It is important to consider whether grey matter contributions to ageing-related differences in sleep neural activity differ under relatively lower sleep pressure conditions, such as during a midday nap (e.g., Borbély, 1982; Mander et al., 2017). Because ageing-related differences in sleep pressure are reduced at midday relative to the start of overnight sleep (Mander

et al., 2017), ageing-related differences in sleep neural activity during a midday nap are less likely to be driven by homeostatic sleep pressure than ageing-related differences in overnight sleep neural activity. Further, ageing-related differences in circadian rhythms interact with nocturnal sleep pressure in ways that could influence sleep neural activity (Münch et al., 2007, 2010). Assessing ageing-related differences in neural activity during midday sleep can therefore help disentangle ageing-related changes in homeostatic sleep pressure from ageing-related changes in basic sleep physiology and circadian sleep governance.

Moreover, naps are of particular interest to ageing-related sleep research, given that naps are prevalent in older adults and have been suggested to be a possible intervention for ageing-related changes in cognition (Mantua & Spencer, 2017). Additionally, from a research perspective, a nap paradigm (i.e., comparing afternoon wake to afternoon sleep bouts) is commonly used to study sleep function as it controls for circadian confounds. We have reported that naps are a microcosm of overnight sleep with regard to ageing-related changes in sleep architecture (Jones & Spencer, 2020; Mantua & Spencer, 2017). Thus, an additional goal of the present study was to understand whether this is true for the topography and neural generators of nap sleep microstructure as well.

1.4 | The present study

We analysed high-density EEG collected from young and older adults during a midday nap, in light of GMV measures extracted from high-resolution structural MRI scans. Our hypothesis was that ageing-related changes in sleep neuroscillatory activity, and the relationships thereof to grey matter, are trait-like changes in sleep physiology rather than state-like changes due to sleep pressure or circadian influence, and would be evident in similar ways during a midday nap as during overnight sleep. Based on previous overnight sleep research, we predicted reductions in the delta, theta, and sigma frequency bands during a midday nap in older relative to younger adults. Moreover, we predicted that these reductions would be largest over frontal scalp for delta, largest over frontocentral scalp for theta and sigma, and that these reductions would lead to an increase in the relative concentration of sigma amplitude over lateral centroposterior scalp. We further predicted that ageing-related reductions in delta and theta during a midday nap would be mediated by grey matter atrophy in frontal cortical regions, and that ageing-related reductions in theta and sigma would be mediated by grey matter

atrophy in the hippocampus. Lastly, following Fogel et al. (2017), we predicted that the relationships between nap neuroscillatory activity and GMV will be moderated by age, such that they are stronger in young adults.

2 | MATERIALS AND METHODS

2.1 | Participants

Data were taken from a larger study on ageing-related changes in sleep and learning; additional analyses of data from this study are reported in Fitzroy, Kainec, Seo, and Spencer (2021). Participants were 26 healthy right-handed young adults (18–31 years, $M = 22.42$, $SD = 2.9$, 12 males) and 21 healthy right-handed older adults (58–75 years, $M = 65.29$, $SD = 5.49$, 11 males). Participants were excluded based on the following criteria: left-handedness; self-reported presence of neurological, psychiatric, cardiac or sleep disorders; use of medications or supplements affecting sleep; excessive napping; caffeine or alcohol consumption; habitual bed time after 12 PM or wake time before 5 AM; and implanted metal or other contraindications for the magnetic resonance imaging (MRI) environment. All older adults were free of self-reported cognitive decline. Standardised cognitive assessments were available for 16 of the older adults as part of study participation within 2 years following the present study. The Mini-Mental State Exam (MMSE; Folstein et al., 1975) was administered to 10 older adults; scores ranged from 27 to 30, all above the typical threshold of 24 for detecting impaired cognition (Mitchell, 2009). The Telephone Interview for Cognitive Status (TICS; Brandt et al., 1988) was administered to seven older adults, all of whom scored within the normal cognitive status range (≥ 30). Notably, behavioral performance on the motor sequencing task did not differ between those for whom cognitive assessments were available and those for whom they were not (see supporting information Section S1.2).

2.2 | Questionnaires

Participants completed a set of standardised questionnaires to assess typical sleep habits, sleep quality, and chronotype. Habitual sleep (past 30 days) was assessed using the Pittsburg Sleep Quality Index (PSQI; Buysse et al., 1989). Typical daytime sleepiness was assessed using the Epworth Sleepiness Scale (ESS; Johns, 1991). Acute subjective sleepiness prior to and following the nap was assessed using the Stanford Sleepiness Scale (SSS; Hoddes et al., 1973). Chronotype was assessed using

the Morningness-Eveningness Questionnaire (MEQ; Horne & Ostberg, 1976). Depressive symptoms were assessed using the Beck Depression Inventory (BDI; Beck et al., 1996). Lastly, information regarding daily life activities affecting sleep (e.g., caffeine intake, exercise, and prior night sleep), dexterity (e.g., musicianship and hand skills), and self-assessed task performance was also collected. Descriptive statistics for questionnaires can be found in Table 1.

2.3 | Procedures

2.3.1 | General procedures

Written informed consent was obtained from participants. Procedures were approved by the Institutional Review Board at the University of Massachusetts, Amherst. Participants were instructed to get quality sleep the night before experimental sessions and to abstain from caffeine and alcohol consumption during experimental days and the prior night.

On the day of the experiment, participants arrived at the lab at approximately 9 AM. After providing informed consent, participants received instructions for the serial reaction time task (SRTT) and then practiced the visuomotor aspects (i.e., random blocks only) of the SRTT in a mock MRI scanner. Participants next completed the SSS, were positioned in the MRI scanner and underwent a high-resolution structural (T1-weighted) brain scan. After the structural scan, participants performed the SRTT in the MRI scanner while functional MRI images were collected. After completing the morning scanner session, participants took a short break including 30 min for lunch in the lab, then had high-density polysomnography (HD-PSG) applied. HD-PSG was recorded

during a 2-h nap opportunity from 1 to 3 PM, which took place in a darkened room similar to a home bedroom environment. At 3 PM participants were awakened, had the HD-PSG montage removed, and were given time to clean up. Participants then performed a second random-only SRTT practice in the mock scanner, completed a second SSS, and returned to the MRI scanner for another high-resolution structural brain scan (diffusion tensor imaging) and to again perform the SRTT during functional imaging. Lastly, standardised questionnaires were administered to assess sleep habits, quality, chronotype, and self-assessment of task performance. Task performance and functional imaging during the task were collected as part of larger multiday protocol and are reported in a parallel manuscript (Fitzroy et al., 2021). Diffusion-weighted images were also collected as part of the larger protocol and are not included in analyses here.

2.3.2 | Task

Participants performed an explicit variant of the SRTT, in which they were aware that there was an underlying pattern in the stimulus sequence but not directly informed what the pattern was. Responses were cued when one of four boxes on a screen display illuminated (black fill turned white). The display was positioned behind the scanner bore and made visible to the participant via an angled mirror mounted to the head coil directly in front of their eyes. Participants rested their non-dominant (left) hand on a response box and were instructed to respond quickly and accurately by pressing the button corresponding to the location of the cue. The boxes flashed at a regular interval (1000 ms) either according to a regular repeating eight-item sequence or randomly in a block design, with 40 flashes (trials) in each block.

TABLE 1 Questionnaire data

	Young adults ($n = 26$)		Older adults ($n = 21$)		Age differences
	n	M (SD)	n	M (SD)	p
Prior night sleep	21	7.21 (1.01)	18	6.97 (1.36)	0.553
PSQI	23	4.78 (2.37)	19	4.58 (1.54)	0.748
ESS	22	7.95 (3.90)	21	7.38 (3.44)	0.611
SSS-1	23	2.48 (0.79)	21	2.14 (0.73)	0.150
SSS-2	23	2.39 (1.08)	21	2.05 (0.80)	0.235
MEQ	23	47.70 (10.43)	16	61.06 (10.29)	**< 0.001**
BDI	17	7.41 (8.00)	17	4.76 (5.25)	0.264

Note: Group means and standard deviations of questionnaire data. Prior night sleep duration is reported in hours. Significant ($p < 0.05$) age differences are highlighted in bold.
Abbreviations: BDI, Beck Depression Inventory; ESS, Epworth Sleepiness Scale; M, mean value; MEQ, Morningness-Eveningness Questionnaire; n, number of participants with available data; PSQI, Pittsburgh Sleep Quality Index; SD, standard deviation; SSS, Stanford Sleepiness Scale (SSS-1: pre-nap; SSS-2: post-nap).

Twelve blocks were presented, organised in six pairs of alternating block types (sequence and random), with a 30-s rest period between the third and fourth block-pairs. Block type was indicated at the start of each block, and participants were instructed to notice and learn any patterns they might observe on sequence blocks.

2.3.3 | High-density polysomnography

HD-PSG data were acquired with reference to FCz using a custom 129-channel cap (Easycap, Herrsching, Germany) and BrainAmp MR plus amplifiers (Brain Products GmbH, Gilching, Germany). The montage consisted of 123 scalp EEG electrodes placed at 10–10 and intermediary locations, 4 electrooculogram (EOG) electrodes placed beside and below the eyes, and 2 electromyogram (EMG) electrodes placed over the zygomatic major and mylohyoid muscles. Data were recorded using a hardware bandpass of 0.1–1000 Hz and digitised at 500 Hz using BrainVision Recorder (Brain Products GmbH, Gilching, Germany). Scalp impedances were reduced below 20 kΩ using high-chloride abrasive gel before the nap.

2.3.4 | MRI data acquisition

Whole-brain images were collected using a Siemens 3T MAGNETOM Skyra scanner (Siemens Healthcare, Erlangen, Germany) with a 20-channel head coil. High-resolution T1-weighted structural scans were acquired in the sagittal plane using a three-dimensional magnetisation-prepared rapid gradient echo (MPRAGE) sequence (TE = 2.26 ms, TR = 1810 ms, TI = 915 ms, FA = 9°, 224 slices, FoV = 224 × 256 × 256 mm^2, voxel size 0.8 × 0.797 × 0.797 mm^3). For 12 young adults and 10 older adults T1 images were collected on the same day as the nap; for the remaining 14 young adults and 11 older adults T1 images were collected 7 days prior to the nap during a data collection session following an identical experimental protocol other than having a wake interval instead of the nap. In all cases the T1 images were collected on the first day of participation in the experiment.

2.4 | Data analysis

2.4.1 | Sleep staging

To identify sleep stages, FCz-referenced HD-PSG recordings were bandpass-filtered offline (0.3 to 35 Hz EEG, 10 to 70 Hz EMG), re-referenced to the contralateral mastoid, then visually scored (30 sec epochs) according to American Academy of Sleep Medicine criteria (Iber, 2007) using the Hume toolbox (Saletin & Greer, 2015).

2.4.2 | Task performance

Performance on the SRTT was quantified separately as reaction time on sequence blocks, random blocks, and the difference between the two (skill learning; i.e., random minus sequence) before and after the nap. Reaction times before the nap were quantified as the median correct reaction time within the appropriate block type, averaged over the final two block-pairs of the pre-nap session. Reaction times after the nap were quantified as the median correct reaction time within the appropriate block type in the second block-pair of the post-nap session. Within random blocks, reaction times were excluded for cues that formed trills (e.g., 1-3-1), runs of three or more (e.g., 1-2-3 or 3-2-1), or had transitional probabilities greater than 0.33 to avoid influence of expectancy-driven facilitation (e.g., Soetens et al., 2004).

2.4.3 | EEG amplitude processing

Motivated by prior work (Dubé et al., 2015; Fogel et al., 2017; Latreille et al., 2019; Mander et al., 2013; Sprecher et al., 2016) and verified by cluster-based permutation analyses in the spectral domain (see supporting information Section S1.1), we analysed time-domain EEG amplitude separately in the delta, theta, and sigma frequency bands. Unfiltered, FCz-referenced recordings were re-referenced to the averaged mastoid and manually inspected for bad channels, and channels identified as bad for a large portion of the recording were spherically interpolated. Bad channel interpolation was necessary for 19 younger adults (number of bad channels: $M = 1.47$, $SD = 0.61$) and 19 older adults (number of bad channels: $M = 2.26$, $SD = 2.56$). Amplitude envelopes were extracted from EEG recordings in the delta (0.5–4 Hz), theta (4–8 Hz) and sigma (12–16 Hz) frequency bands using the filter-Hilbert method (Freeman, 2004). We adopt the frequency-windowed time-domain amplitude approach of the filter-Hilbert method over more common time-windowed spectral amplitude approaches (e.g., short-time Fourier transform) because it allows optimisation of filter designs for each frequency band of interest, and we find that using amplitude envelopes facilitates artefact excision and sleep macrostructure handling.

EEG data were first bandpass-filtered using band-specific filter designs: delta used a second-order Butterworth IIR filter; theta used a Chebyshev Type II filter requiring ≥20-dB attenuation in the stopband (outside 4–9 Hz) and ≤2 dB attenuation in the passband (4.5–8 Hz), and sigma used a 164th-order FIR filter after demeaning the data. Artefactual sections of filtered data were identified automatically for each electrode using band-specific voltage thresholds (delta: ±250 μV; theta/sigma: ±75 μV). Final artefact thresholds were determined through visual inspection of full-recording amplitude envelopes and iterative adjustment. Band-specific amplitude envelopes were created for each electrode by taking the magnitude of the complex analytic signal produced by the Hilbert transform of the bandpass-filtered EEG (i.e., abs (hilbert (EEG.data (ch,:))) in MATLAB). Artefact-free regions of the band-specific amplitude envelopes recorded during the first 60 min of combined NREM2/NREM3 sleep were averaged into non-overlapping 20-s epochs then averaged again across epochs to give a single amplitude measure per combination of frequency band, electrode, and participant. EEG analyses were limited to the first 60 min of NREM2/NREM3 sleep to maximise potential contributions of sleep homeostatic pressure to the sleep EEG, which are largest early in the sleep bout (Münch et al., 2004).

2.4.4 | EEG amplitude statistical analysis

Ageing-related differences in EEG amplitude were assessed using non-parametric cluster-based permutation tests over the topography dimension within each frequency band (Maris & Oostenveld, 2007; Oostenveld et al., 2011). Between-groups independent-samples t values were calculated for amplitude at each electrode, and t values with magnitude greater than the threshold values (corresponding to the 2.5th and 97.5th quantiles of a two-tailed t-test) were considered for cluster inclusion. Sufficiently large t values of the same sign (positive or negative) were clustered by topographical adjacency, defined by a triangulation algorithm applied to a 2D projection of electrode location. Clusters were required to contain at least two electrodes.

A mass score was calculated for each cluster by summing all individual t values contained within. Cluster significance was assessed empirically using a Monte Carlo simulation with 1000 iterations; each cluster observed in the canonical data was assigned a p-value equal to the proportion of randomly shuffled Monte Carlo iterations resulting in a cluster of that magnitude or larger. Cluster significance was evaluated at $\alpha = 0.025$ reflecting the two-tailed nature of the permutation test.

To capture ageing-related changes in both overall neural activity and the relative topography thereof during a nap, the cluster-based permutation testing procedure was completed twice: once to assess absolute EEG amplitude and once to assess topographically relative (i.e., divided by the across-channel mean) EEG amplitude. Dividing by the across-channel mean centers the relative amplitude around 1 and scales it, creating ratios to the overall scalp mean at each electrode and facilitating topography comparisons across age groups with large absolute amplitude differences (e.g., Kurth et al., 2010). EEG amplitude analyses were completed using a combination of EEGLAB (Delorme & Makeig, 2004), ERPLAB (Lopez-Calderon & Luck, 2014), Fieldtrip (Oostenveld et al., 2011) and in-house MATLAB software (PSGpower; https://osf.io/qsryf/).

2.4.5 | GMV processing

GMV was assessed using voxel-based morphometry (VBM). Structural (T1) images were processed with FSL-VBM 1.1 (Douaud et al., 2007, http://fsl.fmrib.ox.ac.uk/fsl/fslwiki/FSLVBM), an optimised VBM protocol (Good et al., 2001) carried out with FSL tools (Smith et al., 2004). Structural images from 21 randomly selected younger adults and all 21 older adults were brain-extracted and grey matter-segmented, then registered to ICBM-152 standard space using non-linear registration (Andersson et al., 2007). The resulting images were averaged and flipped along the x-axis to create a left–right symmetric grey matter template (Figure 1). The subsampling of the young adult cohort was performed to avoid overrepresentation of young adults in the grey matter template; the randomly selected subcohort of 21 young adults did not differ in age, sex, prior night sleep duration, typical daytime sleepiness, pre-nap or post-nap sleepiness, or sleep macrostructure from the full ($n = 26$) cohort of younger adults ($ps > 0.4$). Next, all native grey matter images were non-linearly registered to this study-specific template and modulated to correct for local expansion (or contraction) due to the non-linear component of the spatial transformation (Good et al., 2001). The modulated grey matter images were then smoothed with an isotropic Gaussian kernel with a sigma of 3 mm.

Motivated by the broad ageing-related differences in GMV observed in whole-brain analyses, to facilitate comparisons with behavioral and EEG data, GMV was extracted from several regions of interest (ROIs; Figure 1) expected to contribute to delta, theta, and sigma activity generation during sleep following a motor sequence learning task (Buchmann et al., 2011; Doyon & Benali, 2005; Fogel et al., 2017; Helfrich et al., 2018;
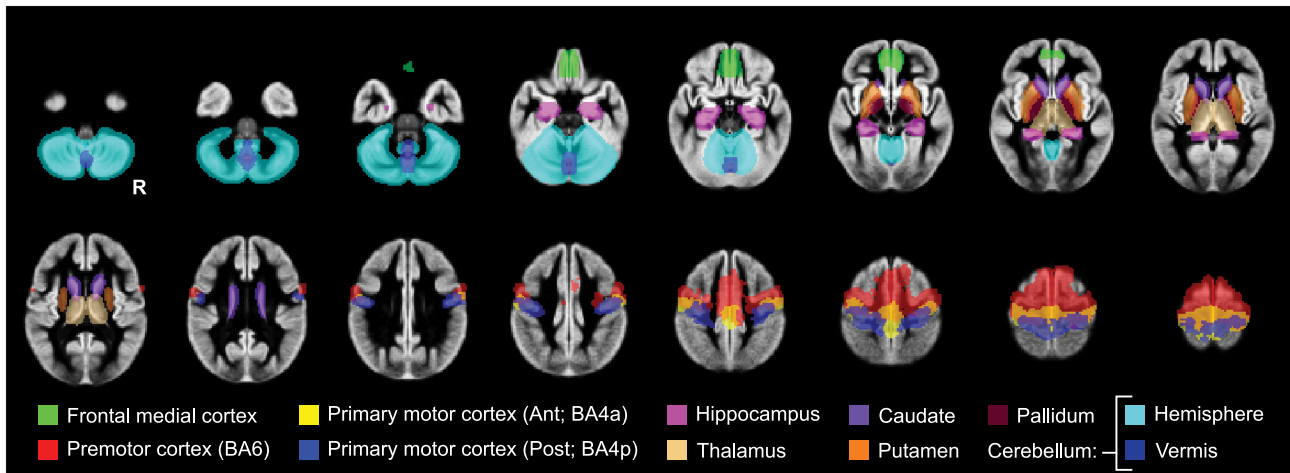
FIGURE 1 Grey matter volume regions of interest (ROIs). Binarised ROI masks extracted from probabilistic atlases are plotted over the symmetric grey matter template created as part of FSL-VBM processing

Mander et al., 2013, 2014; Saletin et al., 2013). GMV was measured separately within frontal medial cortex, premotor cortex (BA6), anterior primary motor cortex (BA4a), posterior primary motor cortex (BA4p), hippocampus, thalamus, caudate, putamen, pallidum, cerebellar hemispheres (lobules I, II, III, IV, V, VI, Crus I, Crus II, VIIb, VIIIa, VIIIb, IX and X), and cerebellar vermis (lobules VI, Crus I, Crus II, VIIb, VIIIa, VIIIb, IX and X). GMV was measured separately in the left and right hemispheres for all ROIs except frontal medial cortex and cerebellar vermis. ROIs were defined using probabilistic atlases: frontal medial cortex was defined using the Harvard–Oxford cortical atlas (Desikan et al., 2006); premotor and primary motor cortices were defined using the Jülich atlas (Eickhoff et al., 2005; Geyer, 2004; Geyer et al., 1996); hippocampal, striatal and thalamic ROIs were defined using the Harvard–Oxford subcortical atlas (Frazier et al., 2005); and cerebellar ROIs were defined using the non-linearly registered probabilistic cerebellar atlas in FSL (Diedrichsen et al., 2009, 2011). Atlas-defined ROIs were binarised by thresholding at a probability of 0.15 or higher. ROI GMV was defined as the mean intensity of non-zero voxels of the modulated, smoothed grey matter images within each ROI.

2.4.6 | GMV statistical analyses

Ageing-related differences in GMV were first assessed using a voxelwise whole-brain general linear modelling approach covarying for estimated total intracranial volume, employing cluster-based permutation analyses with the threshold-free cluster enhancement implemented in FSL's *randomise* (Salimi-Khorshidi

et al., 2011; Winkler et al., 2014). Total intracranial volume was estimated after automatic segmentation in FreeSurfer v6.0.0 (http://surfer.nmr.mgh.harvard.edu/) as a function of the determinant of the transform matrix for atlas alignment (Buckner et al., 2004; Fischl et al., 2002). Additionally, ageing-related differences in mean GMV within each ROI were assessed using multiple linear regression covarying for estimated total intracranial volume, with each ROI analysed in a separate model.

2.4.7 | GMV contributions to ageing-related differences in EEG amplitude

To determine the contributions of ageing-related grey matter atrophy to ageing-related changes in nap EEG amplitude, EEG amplitude measures found to differ with age were entered into regression models testing whether the Age x EEG relationship was mediated and/or moderated by mean GMV within each volumetric ROI. Based on where ageing-related differences in EEG amplitude were observed in whole-scalp analyses, to facilitate comparisons with behaviour and GMV, absolute and topographically relative EEG amplitudes were each averaged within a series of six laterally symmetric spectrotopographic ROIs: frontal delta, occipital delta, frontal theta, occipital theta, frontal sigma, and lateral sigma. The frontal ROIs included AFF1h, AFF2h, F1, Fz, F2, FFC1h, FFC2h and FCz for absolute delta, absolute and relative theta, and absolute and relative sigma; the frontal ROI for relative delta included Fpz, Fp1, Fp2, AFp1, AFp2, AF7 and AF8. The occipital ROIs included PPO1h, PPO2h, POz, PO3, PO4 and Pz for absolute and relative delta and theta. The lateral sigma ROI included electrodes TP7, TTP7h, CP5, CCP5h, CCP6h, CP6, TTP8h

and TP8. Mediation and moderation of ageing-related EEG differences by GMV were assessed separately for each EEG ROI and GMV ROI.

Mediation of a given ageing-related EEG difference by GMV within a given ROI was first screened for using the causal steps method (Baron & Kenny, 1986; MacKinnon et al., 2007), covarying for estimated total intracranial volume (eTIV), then confirmed with bootstrap estimation (Tingley et al., 2014). For causal steps mediation, three regression models were created: a base model with the structure $EEG = \beta_0 + \beta_1(Age) + \beta_2$ (eTIV), a mediator model with the structure $GMV = \beta_0 + \beta_1(Age) + \beta_2(eTIV)$, and an outcome model with the structure $EEG = \beta_0 + \beta_1(Age) + \beta_2(eTIV) + \beta_3(GMV)$. The EEG, Age, eTIV and GMV vectors were centred before being entered into the models. Mediation required that (1) age predict EEG in the base model, (2) age predict GMV in the mediator model, (3) GMV predict EEG in the outcome model, and (4) the age effect estimate (β_1) be reduced in the outcome model relative to the base model. For each mediation identified using the causal steps method, the magnitude and reliability of the average causal mediation effect (ACME) and average direct effect (ADE) were empirically estimated by a bootstrap procedure with 1000 iterations. For significant mediation results ($p_{ACME} < 0.025$), the proportion of the total effect of Age on EEG mediated by GMV ($P_{Mediated}$) was calculated as (ACME + ADE) /ACME.

Moderation of an ageing-related EEG difference by GMV within an ROI was tested using an interaction model covarying for eTIV, with the structure $EEG = \beta_0 + \beta_1(Age) + \beta_2(eTIV) + \beta_3(GMV) + \beta_4(Age*GMV)$. Moderation required that (1) the overall F-test of the interaction model be significant, and (2) the Age*GMV interaction predicts EEG. Interaction p-values were adjusted within each EEG measure using the Benjamini–Hochberg procedure (Benjamini & Hochberg, 1995) to hold false discovery rate at 0.05 while testing multiple grey matter ROIs. For each significant moderation, young adults and older adults were examined separately using follow-up regression models with the structure $EEG = \beta_0 + \beta_1(eTIV) + \beta_2(GMV)$. All regression analyses were performed in R (R Core Team, 2020; RStudio Team, 2018), using add-on packages *mediation* (Tingley et al., 2014) and *reghelper* (Hughes, 2020).

2.4.8 | GMV and EEG amplitude contributions to ageing-related differences in task performance

To assess whether ageing-related grey matter atrophy or changes in nap EEG amplitude contributed to ageing-related changes in task performance, reaction times on the SRTT were considered as dependent variables in mediation and moderation analyses employing the same structure used to evaluate grey matter contributions to ageing-related changes in nap EEG amplitude. The GMV and EEG amplitude predictors in these analyses were the ROI-collapsed measures described in previous sections. No GMV or EEG amplitude measures were found to significantly mediate or moderate any of the reaction time measures, and so these results are not discussed further. Analyses of the behavioral data unto themselves are reported in the supporting information (Section S1.2).

3 | RESULTS

3.1 | Sleep macrostructure characteristics

Young and older adults did not differ in prior night sleep duration, habitual sleep quality (PSQI), typical daytime sleepiness (ESS), pre-nap (SSS-1) or post-nap (SSS-2) acute sleepiness, or depressive symptoms (BDI) (Table 1). Young and older adults did differ in chronotype (MEQ), with young adults typically intermediate type and older adults typically morning type (Table 1). All participants were able to nap, and young and older adults did not differ significantly on nap length or time spent in individual sleep stages (Table 2). Average total sleep time was >100 min in both groups and was not affected by age ($p = 0.27$). Total and percent times spent in NREM1, NREM2, NREM3 and REM also were not affected by age ($ps > 0.1$). Although the groups did not differ significantly on minutes or percent of the nap spent in REM, a higher proportion of young adults reached REM sleep than did older adults (young = 0.88, older = 0.52; $\chi^2 = 5.86$, $p = 0.015$).

3.2 | Ageing-related differences in EEG amplitude

Ageing-related decreases in absolute EEG amplitude, and changes in the relative distribution of amplitude across the scalp, were observed within the delta, theta, and sigma frequency bands during the first 60 min of NREM2/NREM3 in a midday nap. Absolute delta amplitude was lower in older adults than in young adults over most of the scalp; a single significant negative cluster containing 115 electrodes was identified, mass = −378.9, $p = 0.001$ (Figure 2a,c). Additionally, older adults had lower relative delta concentration than young adults over

TABLE 2 Sleep macrostructure statistics

	Young adults (n = 26) M (SD)	Older adults (n = 21) M (SD)	Age differences p
TST (min)	111.19 (14.18)	105.14 (21.33)	0.272
NREM1 (min)	16.12 (13.56)	11.52 (7.76)	0.153
NREM2 (min)	53.15 (16.15)	57.57 (19.18)	0.405
NREM3 (min)	19.08 (15.72)	15.45 (15.67)	0.436
REM (min)	10.19 (8.1)	7.02 (10.72)	0.270
NREM1 (% TST)	15.14 (12.70)	11.61 (8.41)	0.260
NREM2 (% TST)	47.72 (13.17)	54.35 (13.75)	0.102
NREM3 (% TST)	16.52 (13.27)	13.63 (13.24)	0.461
REM (% TST)	8.90 (6.71)	6.29 (9.36)	0.291

Abbreviations: M, mean value; NREM, non-rapid eye movement; REM, rapid eye movement; SD, standard deviation; TST, total sleep time.
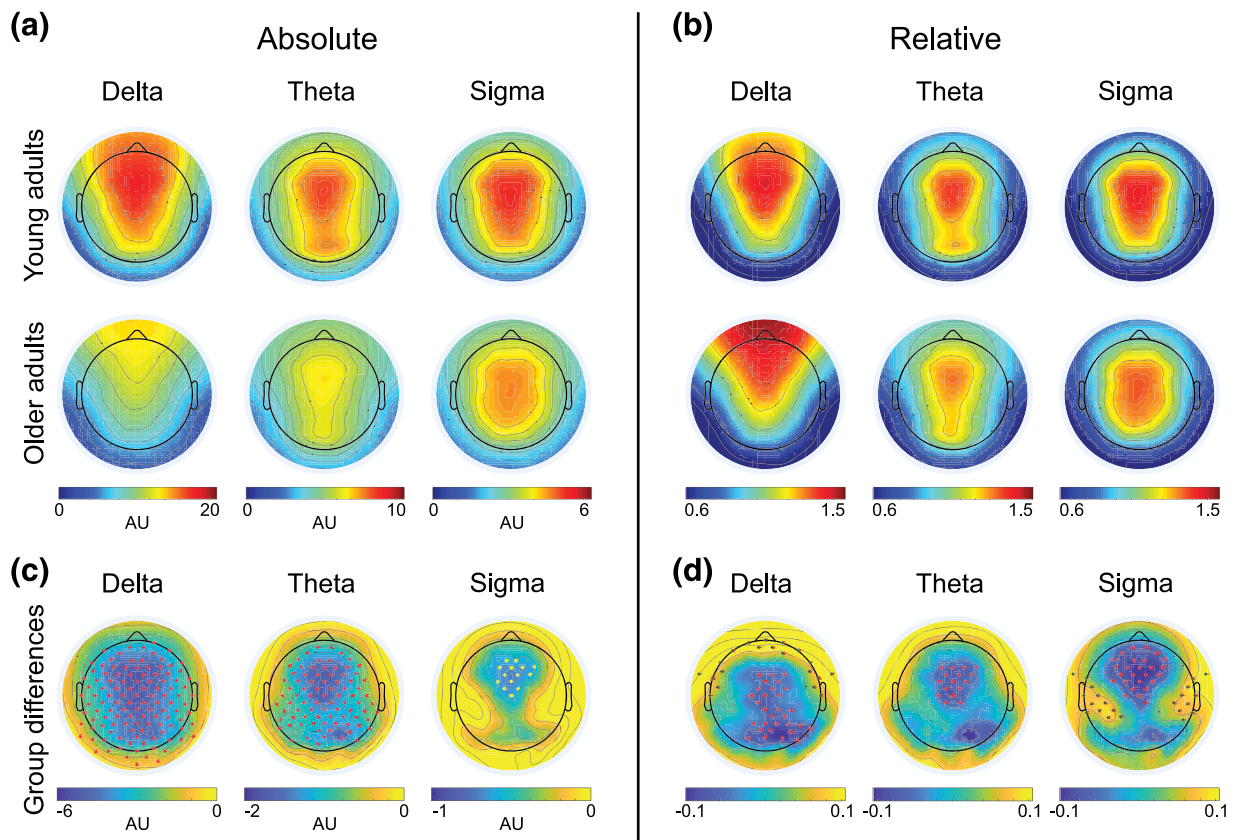

FIGURE 2 Ageing-related differences in electroencephalogram (EEG) amplitude. (a, b) EEG amplitude in the delta (0.5–4 Hz), theta (4–8 Hz), and sigma (12–16 Hz) frequency bands is shown separately for young and older adults. Absolute amplitude is shown in (a); topographically relative amplitude (i.e., divided by the mean of all channels) is shown in (b). Absolute amplitude is reported in arbitrary units (AU) because the analytic amplitude is unitless, but in the context of scalp EEG these arbitrary units are akin to μV; relative amplitude is unitless because it is a ratio. (c, d) Group differences in time-domain absolute (c) and topographically relative (d) amplitude are plotted in colour across the scalp. Electrodes contained in significant ($p < 0.025$) clusters are plotted in red (negative clusters; older < young) or dark green (positive clusters; older > young). Electrodes contained in marginal ($0.025 \leq p \leq 0.05$) clusters are plotted in yellow (negative clusters; older < young)

medial frontocentral and posterior scalp, as indicated by a single significant negative cluster containing 30 electrodes, mass = −79.3, $p = 0.002$ (Figure 2b,d). However, older adults also had higher relative delta concentration than young adults over far frontal scalp, as indicated by a single significant positive cluster containing 20 electrodes, mass = 65.5, $p = 0.005$ (Figure 2b,d).

Absolute theta amplitude was lower in older adults than in young adults over a broad scalp region; a single significant negative cluster containing 83 electrodes was identified, mass = −239.9, $p = 0.012$ (Figure 2a,c). Additionally, older adults had lower relative theta concentration than young adults over medial frontocentral scalp, as indicated by a single significant negative cluster containing 16 electrodes, mass = −40.2, $p = 0.019$ (Figure 2b,d).

There was some evidence that absolute sigma amplitude was lower in older adults than in young adults over medial frontocentral scalp; a single marginal negative cluster containing 14 electrodes was identified, mass = −31.1, $p = 0.031$ (Figure 2a,c). Further, older adults had lower relative sigma concentration over medial frontocentral scalp, as indicated by a single significant negative cluster containing 26 electrodes, mass = 80.2, $p = 0.002$ (Figure 2b,d). Additionally, older adults had higher relative sigma concentration over lateral centroposterior scalp regions, as indicated by two significant positive clusters: one over left lateral centroposterior scalp containing 12 electrodes, mass = 42.9, $p = 0.015$, and another over right lateral centroposterior scalp containing 10 electrodes, mass = 37.4, $p = 0.024$ (Figure 2b,d).

3.3 | Ageing-related differences in GMV

As predicted, young adults had greater GMV than older adults across most brain regions (Figure 3). This was reflected by a single large cluster in permutation testing with a centre of gravity located near the thalamic midline (Figure 3 and Table S1). Older adults had greater GMV in small sections of dorsal right caudate and medial right thalamus, as reflected by small clusters with maxima located in these regions (Figure 3 and Table S1). ROI-extracted mean GMV measures were consistent with the cluster-based permutation results; in regression models covarying for estimated total intracranial volume, ageing-related reductions in mean ROI GMV were significant for all ROIs except for right thalamus (Table 3).

3.4 | GMV contributions to ageing-related differences in EEG amplitude

3.4.1 | Delta

Ageing-related reductions in absolute frontal and occipital delta amplitude were mediated by GMV loss in frontal medial cortex, the anterior and posterior divisions of left primary motor cortex, and left thalamus (Figure 4 and Table S2). The indirect effect via GMV loss in frontal medial cortex accounted for 0.71 of absolute delta reduction over frontal scalp ($p = 0.006$) and 0.79 over occipital scalp ($p < 0.001$). The indirect effect via grey matter loss in anterior left primary motor cortex
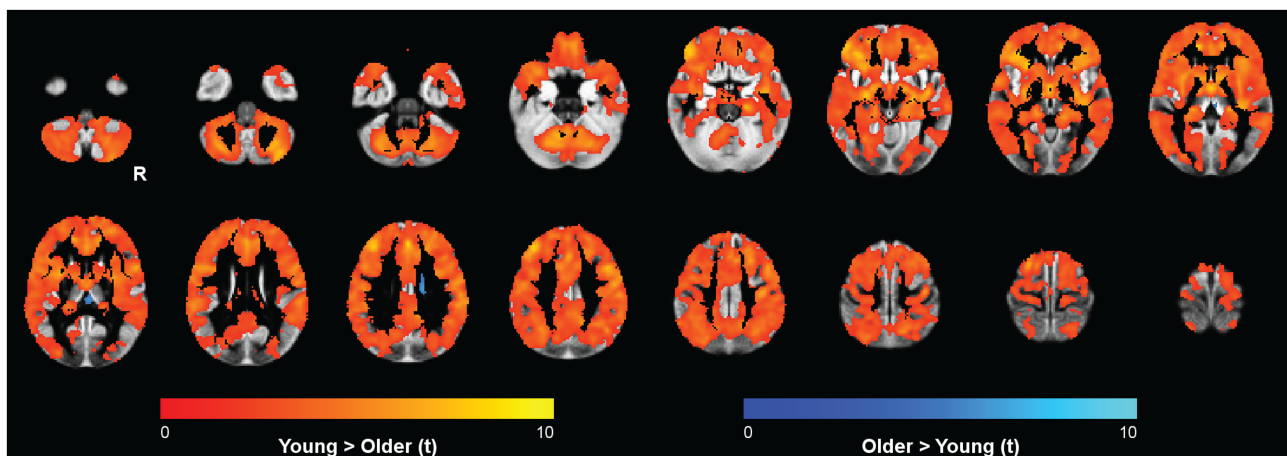

FIGURE 3 Ageing-related differences in grey matter volume. Effect sizes (t) for clusters identified in voxelwise whole-brain permutation testing using the threshold-free cluster enhancement are plotted for the young > older contrast (red-yellow) and the older > young contrast (blue-cyan). These models included estimated total intracranial volume as a covariate. Clusters are overlaid on the symmetric grey matter template created during FSL-VBM processing

TABLE 3 Ageing-related differences in mean within-ROI grey matter volume

ROI	Hem	EMM$_{YA}$	EMM$_{OA}$	β_{Age}	p_{Age}
Frontal medial cortex	-	0.574	0.465	0.109	**<0.001**
Premotor cortex	L	0.383	0.325	0.059	**<0.001**
	R	0.353	0.301	0.053	**<0.001**
Primary motor cortex (anterior)	L	0.336	0.298	0.037	**0.002**
	R	0.310	0.276	0.034	**0.002**
Primary motor cortex (posterior)	L	0.349	0.295	0.054	**<0.001**
	R	0.337	0.280	0.057	**<0.001**
Hippocampus	L	0.567	0.531	0.036	**0.027**
	R	0.559	0.528	0.032	**0.011**
Thalamus	L	0.355	0.328	0.027	**0.005**
	R	0.362	0.349	0.013	0.143
Caudate	L	0.402	0.356	0.046	**0.001**
	R	0.378	0.343	0.035	**0.012**
Putamen	L	0.358	0.309	0.049	**<0.001**
	R	0.394	0.344	0.050	**<0.001**
Pallidum	L	0.162	0.137	0.026	**<0.001**
	R	0.186	0.154	0.031	**<0.001**
Cerebellum (hemisphere)	L	0.459	0.414	0.045	**<0.001**
	R	0.452	0.411	0.041	**<0.001**
Cerebellum (Vermis)	-	0.496	0.448	0.048	**0.002**

Note: The predictive power of age group for grey matter volume was tested separately in each ROI using linear regression models that included estimated total intracranial volume as an additional predictor. Significant ($p < 0.05$) age group effects are highlighted in bold.

Abbreviations: EMM, estimated marginal mean; Hem, hemisphere; L, left; OA, older adults; R, right; ROI, region of interest; YA, young adults.
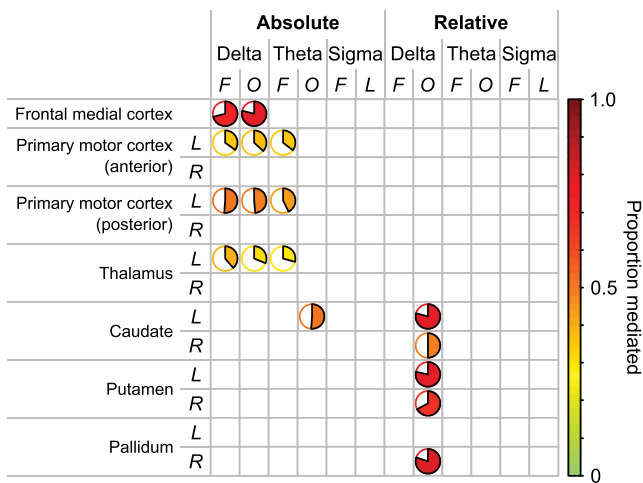

FIGURE 4 Mediation results. The proportion of the total effect accounted for by the estimated indirect effect (i.e., total effect/average causal mediation effect [ACME]) is plotted for each electroencephalogram (EEG) measure in which ageing-related changes were significantly mediated by mean grey matter volume in the specified region of interest (ROI). For clarity, grey matter ROIs were tested but did not significantly mediate ageing-related changes in any EEG measures (i.e., premotor cortex, hippocampus, cerebellar hemispheres, cerebellar vermis) are omitted

accounted for 0.35 of absolute delta reduction over frontal scalp ($p = 0.020$) and 0.37 over occipital scalp ($p = 0.010$), and the indirect effect via grey matter loss in posterior left primary motor cortex accounted for 0.51 of absolute delta reduction over frontal scalp ($p < 0.001$), and 0.49 over occipital scalp ($p = 0.004$). The indirect effect via GMV loss in left thalamus accounted for 0.39 of the reduction over frontal scalp ($p = 0.004$) and 0.31 over occipital scalp ($p = 0.016$). Additionally, ageing-related reductions in relative occipital delta were mediated by GMV loss in multiple striatal regions (Figure 4 and Table S2), specifically bilateral caudate (left: P$_{Mediated}$ = 0.79, $p < 0.001$; right: P$_{Mediated}$ = 0.50, $p = 0.010$), bilateral putamen (left: P$_{Mediated}$ = 0.79, $p < 0.001$; right: P$_{Mediated}$ = 0.67, $p = 0.004$), and right pallidum (P$_{Mediated}$ = 0.80, $p = 0.006$). Similar to Mander et al. (2013), we found that ageing-related differences in delta amplitude were not mediated by GMV loss in the hippocampus ($ps > 0.5$).

In addition to being mediated by frontal medial cortical, primary motor cortical, thalamic, and striatal GMV, ageing-related differences in delta amplitude were moderated by GMV in the putamen (Figure 5a and
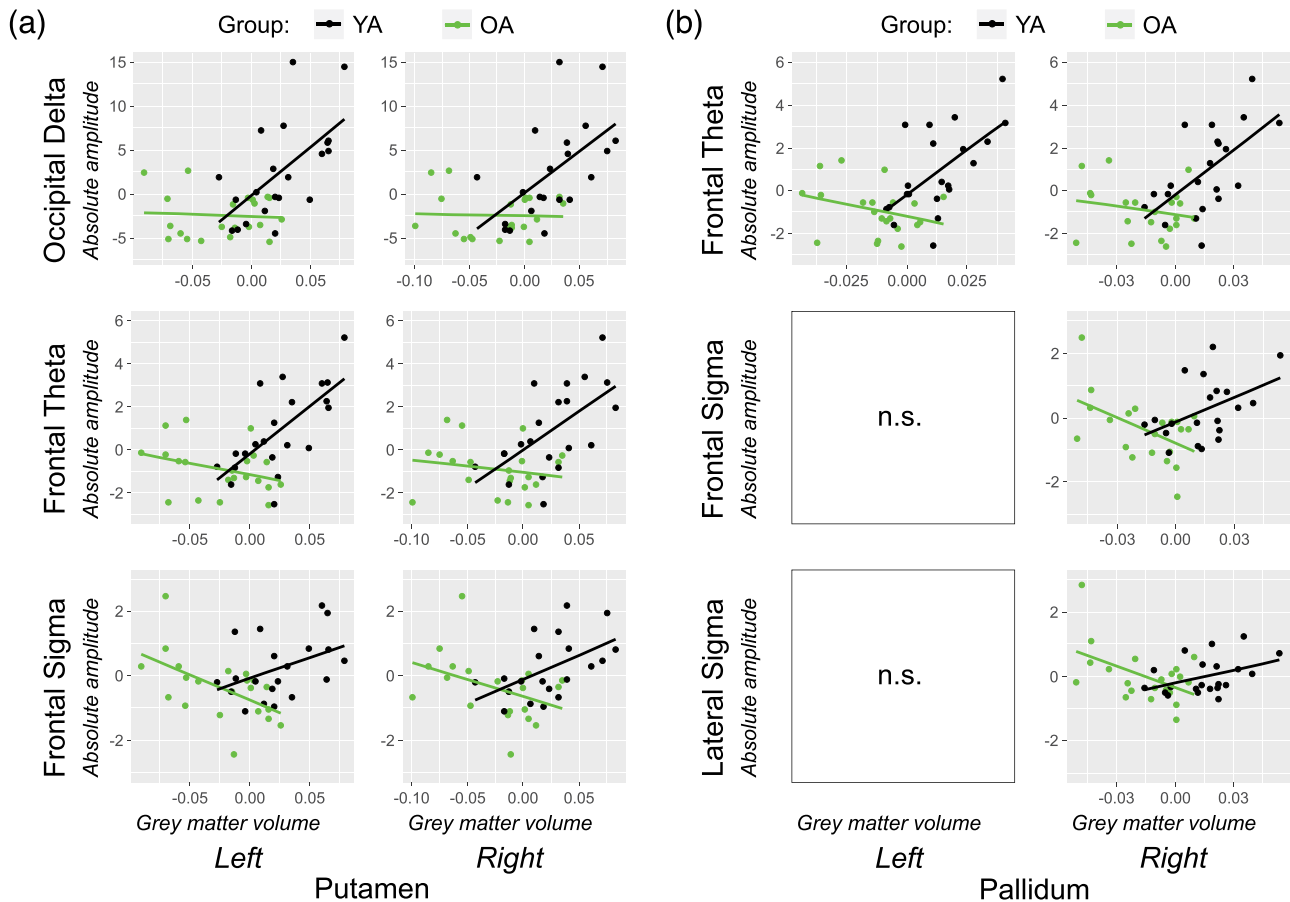
FIGURE 5 Moderation results. Electroencephalogram (EEG) amplitude is plotted against grey matter volume for all comparisons in which the relationship was significantly moderated by age. EEG and grey matter volume vectors were mean-centred prior to entering into the regression models, which is reflected here as data ranges surrounding zero. Y-axis units are arbitrary because the analytic amplitude is unitless, but the arbitrary units are comparable with μV in the context of scalp EEG. X-axis units are the proportion of voxel volume containing grey matter after modulation and smoothing, averaged across non-zero voxels within the specified region of interest (ROI). YA = young adults; OA = older adults

Table S3). Specifically, absolute occipital delta was interactively predicted by age and GMV in bilateral putamen (left: $\beta = 116.10$, $p = 0.003$; right: $\beta = 106.40$, $p = 0.005$), reflecting a positive relationship in young adults only between absolute occipital delta and bilateral putamen GMV.

3.4.2 | Theta

Similar to delta, ageing-related reductions in absolute frontal theta amplitude were mediated by GMV loss in the anterior and posterior divisions of left primary motor cortex, and in left thalamus (Figure 4 and Table S2). The indirect effect via grey matter loss in anterior left primary motor cortex accounted for 0.36 of absolute theta reduction over frontal scalp ($p = 0.004$), and the indirect effect via grey matter loss in posterior left primary motor cortex accounted for 0.43 of absolute theta reduction over

frontal scalp ($p = 0.016$). The indirect effect via grey matter loss in left thalamus accounted for 0.29 of absolute theta reduction over frontal scalp ($p = 0.022$). Additionally, ageing-related reductions in absolute theta amplitude were mediated by GMV loss in left caudate (Figure 4 and Table S2), with the indirect effect accounting for 0.51 of the reduction over occipital scalp ($p = 0.016$). Lastly, though it did not reach our criteria for significance, we observed some evidence that ageing-related reductions in relative frontal theta amplitude were mediated by GMV loss in left hippocampus ($p = 0.070$; Table S2), with the indirect effect accounting for 0.24 of relative frontal theta reduction. For comparison, ageing-related hippocampal GMV loss showed no evidence of mediating ageing-related changes in any other EEG measure ($ps > 0.2$).

In further similarity to delta, ageing-related changes in theta amplitude were moderated by GMV in the striatum. Specifically, absolute frontal theta was interactively

predicted by age and GMV in bilateral putamen (Figure 5a; left: $\beta = 56.37$, $p < 0.001$; right: $\beta = 46.89$, $p = 0.001$) and bilateral pallidum (Figure 5b; left: $\beta = 111.79$, $p = 0.001$; right: $\beta = 94.02$, $p = 0.001$). These interactions reflected positive relationships in young adults only between absolute frontal theta amplitude and striatal GMV (Figure 5 and Table S3).

3.4.3 | Sigma

Ageing-related reductions in sigma amplitude were not mediated by GMV in any of the regions investigated (ps > 0.025). However, GMV in striatal regions had multiple moderating effects on ageing-related reductions in sigma amplitude. Ageing-related differences in absolute frontal sigma were moderated by GMV in bilateral putamen and right pallidum (Figure 5 and Table S3), reflecting a general pattern of negative relationships between absolute frontal sigma and striatal GMV in older adults but positive relationships between these measures in young adults. The negative relationship in older adults was significant for left putamen ($p = 0.014$) and right pallidum ($p = 0.020$) and approached significance for right putamen ($p = 0.093$); the positive relationship in young adults was significant for right putamen ($p = 0.017$) and right pallidum ($p = 0.027$). Absolute lateral sigma reflected a similar crossover interaction of age and GMV in right pallidum (Figure 5b and Table S3), with older adults showing a negative relationship between these measures ($p = 0.016$) but young adults showing some evidence of a positive relationship ($p = 0.055$).

4 | DISCUSSION

Our results replicate in a midday nap previous reports from overnight sleep of ageing-related changes in NREM delta, theta, and sigma amplitude and topography, and that ageing-related grey matter atrophy in frontal cortical regions mediates a large proportion of ageing-related reductions in sleep delta activity. These replications in a nap design clearly indicate that these effects are driven by trait-like ageing-related changes in the physiological mechanisms of sleep rather than by state-like ageing-related changes in sleep pressure or circadian rhythmicity. Additionally, we novelly demonstrate that grey matter atrophy in primary motor cortex, thalamus, and striatal regions mediates ageing-related reductions in NREM delta and theta activity after performance of a motor sequence learning task, suggesting that these brain regions contribute to delta and theta generation following activation during motor sequence learning. Lastly, we

demonstrate an age dependence of the relationships between putamen and pallidum GMV and NREM delta, theta, and sigma activity, suggesting that sleep neuroscillatory activity following motor sequence learning in young adults is resource-bound by striatal GMV and that older adult brains partially compensate for striatal atrophy by increasing sigma generation.

4.1 | Ageing-related changes in sleep physiology

As predicted, we observed ageing-related reductions in neuroscillatory activity in the delta, theta, and sigma frequency bands during a midday nap. In agreement with previous research examining high-density EEG during overnight sleep (Sprecher et al., 2016), the reductions in absolute delta and theta amplitude were topographically broad but largest over medial frontocentral scalp regions, and the reduction in absolute sigma amplitude was topographically constrained to medial frontocentral scalp only. We likewise replicate ageing-related reductions in topographically relative theta and sigma amplitude constrained to medial frontocentral scalp and an ageing-related increase in topographically relative sigma amplitude over lateral centroposterior scalp. This concordance between our findings during a midday nap and Sprecher et al.'s (2016) findings from overnight sleep indicates that these ageing-related changes in sleep delta, theta, and sigma activity represent changes in basic trait-like aspects of sleep physiology rather than changes in homeostatic sleep pressure or other circadian-linked state-like variables.

We additionally report an ageing-related reduction in topographically relative delta amplitude over frontocentral and posterior scalp coupled with an increase in topographically relative delta amplitude over the most frontal scalp. Sprecher et al. (2016), who did not find this result, employed a correlational design across age, revealing changes that progress linearly from 18 to 64 years old. Our point comparison between the extremes of that age range would additionally reveal non-linear ageing-related effects, including changes that do not onset until later in life, especially given that our age range extended to 75 years old. Through this lens, our increase in relative delta frontality in older adults represents an effect of later ageing rather than a nap-specific effect. Supporting this interpretation, an increase in relative delta frontality for older adults relative to younger adults during overnight sleep is evident in previously reported lower density EEG data; in the study by Dubé et al. (2015), ageing-related decreases in slow wave density and amplitude, both of which would contribute

to delta-band activity, were smaller over far frontal scalp than over frontal, central, and posterior scalp, leading to an increase in relative frontality (Dubé et al., 2015, Figure 2). Alternatively, it is possible that the increase in relative delta frontality we observed in older adults during a midday nap is due to circadian differences in EEG amplitude. Older adults in a forced-desynchrony paradigm showed increased broadband (including delta) EEG amplitude during the biological day relative to the biological night (Münch et al., 2010); it is possible that generally higher EEG amplitudes during the midday nap period in the present study increased signal dynamic range in a manner that revealed an ageing-related increase in relative delta frontality that was too small to observe in prior overnight work. Future studies could distinguish these trait-like and state-like interpretations by examining ageing-related changes in relative delta frontality during nap and overnight sleep in the same individuals.

Interestingly, despite previous reports of altered nap macrostructure in older adults (Baran et al., 2016; Fogel et al., 2017; Mantua & Spencer, 2017), we did not observe significant ageing-related differences in total time spent asleep or in any specific sleep stage. This may suggest that our older adult cohort was healthier than the general ageing population, perhaps reflecting a selection bias due to the lengthy experimental protocol. However, in agreement with prior findings of reduced REM during naps in older adults compared with younger adults (Baran et al., 2016; Fogel et al., 2017), a smaller proportion of older adults reached REM during their nap than did young adults. Additionally, though the differences did not reach significance, older adults spent less time in REM and NREM3 and more time in NREM2, leading to a marginal ($p = 0.10$) ageing-related increase in NREM2 as a percentage of total sleep time. This is consistent with past reports of older adult naps being relatively higher in NREM than REM compared with young adult naps (Baran et al., 2016; Fogel et al., 2017). Moreover, our observation of robust ageing-related differences in sleep microstructure in the absence of clear macrostructural differences points to the sensitivity of microstructural measures to ageing-related changes in sleep, highlighting the utility of these measures in assessing sleep health.

4.2 | Ageing-related changes in brain structure

We observed clear ageing-related decreases in GMV across the majority of the brain when controlling for estimated total intracranial volume, as predicted by multiple previous studies (Abe et al., 2008; Good et al., 2001;

Taki et al., 2004). These decreases were evident both as a widespread cluster in the whole-brain analysis and individually within every ROI investigated except for the right thalamus. Although two small regions in right caudate and thalamus were identified in the whole-brain analysis as having increased GMV in older adults, mean GMV was not increased in older adults in either of these ROIs. For this reason, and because ageing-related reductions in caudate and thalamus volume have been clearly demonstrated previously (Cherubini et al., 2009; Gunning-Dixon et al., 1998; Raz et al., 2003), we do not consider these small findings to be meaningful.

4.3 | Relationships between ageing-related changes in brain structure and sleep physiology

4.3.1 | Delta

In agreement with past findings from overnight sleep (Latreille et al., 2019; Mander et al., 2013), we observed that GMV loss in frontal medial cortex mediated a large proportion (0.71) of ageing-related reductions in absolute NREM delta amplitude during a nap. This is consistent with source localisation work indicating a pre-eminent role for frontal medial cortex in slow wave generation (Bersagliere et al., 2018), and indicates that frontal medial cortex involvement in ageing-related delta reductions is not a function of ageing-related differences in sleep pressure or circadian rhythmicity. Further, participants in the present study performed a procedural learning task (SRTT) prior to sleep, whereas participants in Mander et al. (2013) performed a declarative learning task (word pair task). The observation of frontal medial cortex mediation of delta amplitude during sleep following these disparate learning tasks suggests that the role of frontal medial cortex in slow wave generation is not dependent on the specific brain regions activated prior to sleep.

We further observed that GMV loss in left primary motor cortex and left thalamus mediated ageing-related reductions in absolute delta amplitude over both frontal and occipital scalp during a nap. Such a relationship was not observed for these brain regions in previous work examining grey matter contributions across the entire cortex to ageing-related changes in overnight NREM delta-band activity (Dubé et al., 2015; Latreille et al., 2019). No cognitive task was performed prior to sleep in the study jointly reported by Dubé et al. (2015) and Latreille et al. (2019), whereas a motor sequence learning task (SRTT) was performed prior to the nap in the current study. Given clear prior evidence of primary motor cortex and thalamus involvement in motor

sequence learning (Doyon & Ungerleider, 2002; Exner et al., 2001; Nitsche et al., 2003), we interpret these mediating relationships as being related to performing the SRTT prior to sleep and therefore dependent on the specific brain regions activated prior to sleep. Notably, the sole previous study examining grey matter contributions to ageing-related changes in sleep delta activity following a learning task (Mander et al., 2013) focused exclusively on grey matter in frontal medial cortex, which would have precluded observation of grey matter contributions from other task-related brain regions.

The left-lateralisation of the thalamus delta mediation likely reflects the left-lateralisation of ageing-related thalamic GMV reductions observed in our cohort. However, the left-lateralisation of the primary motor cortex delta mediation is unexplainable by ageing-related differences in primary motor cortex GMV, which were bilateral. The left-lateralisation of the primary motor cortex delta mediation is therefore likely to be task-related. The lateralisation of this relationship to the left hemisphere is counterintuitive; our participants used their left hand to perform the SRTT, which would be expected to activate contralateral right primary cortex during motor sequence learning (Doyon & Ungerleider, 2002). Our results may then suggest a local sleep-like increase in sleep delta activity in the right primary motor cortex following activation of right primary motor cortex during the left-handed SRTT. Such a state-like increase in right hemisphere delta activity could obscure the right hemisphere component of a bilateral trait-like contribution of primary motor cortex GMV to ageing-related absolute delta reductions, leading to the left-lateralised mediation that we observed.

We additionally observed mediation of ageing-related reductions in relative occipital delta by bilateral caudate, bilateral putamen and right pallidum GMV, and moderation of absolute occipital delta by bilateral putamen GMV. No such relationships were reported in the previous study investigating subcortical GMV contributions to ageing-related changes in overnight sleep delta following no cognitive task (Latreille et al., 2019), and other work investigating grey matter contributions to sleep delta activity has not examined subcortical GMV (Dubé et al., 2015; Mander et al., 2013). The striatum is active during motor sequence learning tasks like the SRTT performed prior to sleep by participants in the present study (Doyon et al., 1997; Doyon & Ungerleider, 2002; Fitzroy et al., 2021; Fogel et al., 2014). The striatal GMV contributions to ageing-related reductions in relative occipital delta observed in the current study are therefore likely related to performing the SRTT, rather than nap-related differences in sleep pressure or circadian control, reflecting contributions from striatal regions to

delta generation during sleep following a motor sequence learning task. This interpretation would suggest that delta generation following motor sequence learning is resource-bound in young and older adults by striatal GMV and that this resource limiting is stronger in young adults for the putamen. This hypothesis is consistent with prior evidence that young adults advance motor sequence learning to a putamen representation more quickly during encoding than older adults (King et al., 2017; Fitzroy et al., 2021). Further, the observation of striatal mediation of ageing-related differences in relative delta topography rather than absolute delta amplitude is consistent with qualitatively different neural generators rather than reduced activity in identical generators, as would be expected following qualitatively different brain region activation due to ageing-related differences in encoding depth. Moreover, this resource-bound hypothesis is consistent with previous evidence that motor sequence learning is impaired in Parkinson's disease patients with bilateral striatal disruption (Doyon et al., 1997).

4.3.2 | Theta

Similar to previous work investigating grey matter atrophy contributions to ageing-related reductions in NREM theta during overnight sleep (Latreille et al., 2019), we observed a mediation of ageing-related reductions in NREM theta amplitude during a midday nap by GMV. Unlike Latreille et al. (2019), who observed mediation of NREM occipital theta reductions by cortical thinning in right lateral occipital cortex but not in subcortical regions, we observed mediation of NREM frontal theta reductions by grey matter atrophy in left primary motor cortex, left thalamus, and left caudate. Additionally, we provide the first evidence, to our knowledge, that the relationship between NREM theta amplitude and striatal GMV is moderated by age, with young adults showing a clear positive linear relationship between absolute frontal theta and bilateral putamen and pallidum GMV, but older adults showing no clear relationship between these factors. As was the case for delta, we posit that the contributions of motor cortical, thalamic, and striatal GMV to ageing-related reductions in NREM theta observed in the present study, which included an SRTT before sleep, but not by Latreille et al. (2019), who included no cognitive task before sleep, reflect contributions to NREM theta by brain regions that were activated during motor sequence learning prior to sleep. Moreover, we interpret the moderation results to indicate that for the putamen and pallidum, this link between pre-sleep activation and NREM theta activation is stronger in young adults.

In addition to the delta-like mediation of ageing-related reductions in NREM theta by neocortical, thalamic and striatal grey matter, our data provide a suggestion that ageing-related changes in theta activity may be mediated by allocortical GMV. Specifically, we found marginal evidence ($p = 0.070$) that ageing-related reductions in relative frontal theta amplitude were mediated by GMV in the left hippocampus. Although this effect did not meet our significance criterion, it was closer to that threshold than any other mediating effect of hippocampal GMV on EEG amplitude ($ps > 0.2$). This marginal ageing-related finding is consistent with the hypothesis of Campbell and Feinberg (2009), based on adolescent data, that NREM theta activity reflects greater contributions from allocortical generators than does NREM delta activity, suggesting that NREM theta may reflect contributions from allocortical generators across the lifespan.

4.3.3 | Sigma

Consistent with Fogel et al. (2017), we observed age-dependent predictive relationships between GMV in multiple brain regions involved in motor sequence learning and EEG activity in the sigma frequency band during a midday nap following a motor sequence learning task. However, the network of sigma-predictive regions observed in the present study differs from that reported by Fogel and colleagues. Fogel et al. (2017) report age-dependent predictability of spindle duration by GMV in the left cingulate and parietal cortices, right supplemental motor area, left hippocampus, and left cerebellum, whereas we observe age-dependent predictability of absolute sigma amplitude by GMV in bilateral putamen and right pallidum. Notably, all of these brain regions are activated during motor sequence learning (Doyon et al., 2003; Doyon & Benali, 2005; Doyon & Ungerleider, 2002; Janacsek et al., 2020), suggesting that the age-dependent predictive relationships observed in both studies reflect age-dependent contributions of these brain regions to sigma activity after activation during motor sequence learning.

The network differences in age-dependent predictability of sigma activity by GMV observed between Fogel et al. (2017) and the present study are likely due to the specific motor sequence learning tasks performed before sleep. The present study employed an SRTT in which the sequence to be learned was not known by the participant, whereas Fogel et al. (2017) employed a task in which the participant was given an explicit sequence to practice. A recent meta-analysis demonstrates that basal ganglia activation during the SRTT is specific to sequence learning, whereas cerebellar activation is related to other aspects of the motor task (Janacsek et al., 2020); the observation of striatal involvement in the present study, which required learning an implicit sequence, and cerebellar involvement by Fogel et al. (2017), which required speeded motor performance of a known sequence, maps directly to this dichotomy. Additionally, it is possible that consolidation of explicit motor sequence learning is more hippocampal-dependent, which would explain why hippocampal grey matter predicted sleep sigma after practicing a specified motor sequence (Fogel et al., 2017) but not after the SRTT in the present study. This task-specificity of GMV prediction of sleep sigma activity supports the hypothesis that regional variation in spindle generators is a function of pre-sleep learning. Alternatively, it is possible that the network differences observed between the present study and Fogel et al. (2017) result from different methods of quantifying sigma activity. We took an aggregate amplitude measure of sigma frequency activity, which reflects the duration and amplitude of both slow and fast spindles as well as non-spindle activity between 12 and 16 Hz, whereas Fogel et al. (2017) separately assessed spindle duration, density and amplitude for slow and fast spindles. Future work could distinguish these interpretations by assessing both aggregate and specific measures of spindle activity following motor sequence learning tasks of varying explicitness.

The age dependence of sigma predictability by striatal GMV in the present study was driven by a combination of positive correlations in young adults and negative correlations in older adults, whereas the age dependence of sigma predictability by hippocampal and cerebellar GMV reported by Fogel et al. (2017) was driven by positive correlations in young adults alone. The positive correlations observed in young adults in both studies suggest that sigma generation is resource-bound in young adult brains by GMV in the striatum following implicit motor sequence learning and by hippocampal and cerebellar GMV following explicit motor sequence learning. Conversely, the negative relationships observed in older adults in the present study suggest that in the presence of striatal atrophy, older adult brains compensate by producing more sigma activity. Such compensation implies that the striatum plays an integral role in the function of sigma activity during post-motor learning sleep and also that increased activation of sigma generators can forestall loss of function up to at least some level of atrophy. Future work could investigate the levels of atrophy in these brain regions at which compensatory sigma is no longer able to maintain function, which could explain some of the degradative effects of ageing on sleep-dependent memory consolidation (e.g., Fogel et al., 2014; Spencer et al., 2007).

4.4 | Limitations

Ageing-related changes in head anatomy and physiology unrelated to neural activity could alter current flow in a manner that causes changes in the scalp-recorded EEG. We control for potential overall effects of head size on scalp EEG by including estimated total intracranial volume, a proxy for head size (Buckner et al., 2004), as a covariate in our regression models. Additionally, ageing-related changes in head conductivity as a function of brain shrinkage and cerebrospinal fluid increases are insufficient to explain ageing-related scalp EEG power reductions (He et al., 2021). Further, changes in skull and scalp thickness do not have appreciable contributions to ageing-related changes in scalp-recorded EEG, as skull thickness does not change substantially during healthy ageing and scalp thickness changes with ageing are variable (Albert et al., 2007; He et al., 2021; Lynnerup, 2001).

A recent meta-analysis does suggest that the brain-to-skull conductivity ratio may increase, reflecting a skull conductivity decrease, during healthy ageing (Goncalves et al., 2003; McCann et al., 2019). This could explain reductions in scalp EEG power in older relative to young adults. However, separate modelling efforts have determined skull connectivity to reach a steady state in early adulthood and remain unchanged with healthy ageing (Wendel et al., 2010), which would argue against this possibility. Nevertheless, future work using invasive methods would clarify the contributions of potential ageing-related changes in skull conductivity to ageing-related changes in sleep EEG amplitude as recorded at the scalp.

5 | CONCLUSIONS

Ageing-related reductions in sleep neuroscillatory activity, and mediation of ageing-related delta reductions by frontal medial cortex atrophy, are driven by changes in the physiological mechanisms of sleep rather than by changes in sleep pressure or circadian rhythmicity. Additionally, during sleep following a motor sequence learning task, atrophy in cortical, thalamic, and striatal regions supporting motor sequence learning mediates ageing-related reductions in delta and theta activity; striatal GMV limits delta, theta, and sigma activity in young adults; and striatal atrophy induces compensatory sigma activity in older adults. These findings support the hypothesis that the regional distribution of sleep neuroscillatory activity reflects the regional distribution of prior-to-sleep neural activity (e.g., Huber et al., 2004), which could represent a systems-level analogue of the

reactivation known to occur in the hippocampus during sleep as part of memory consolidation (Eichenlaub et al., 2020; Wilson & McNaughton, 1994). Overall, our results illustrate clear relationships between changes in brain structure and sleep physiology during healthy ageing, which can serve as baseline comparisons for future work investigating how these processes change during pathological ageing.

CONFLICT OF INTEREST
The authors have no conflicts of interest to disclose.

ETHICS STATEMENT
Procedures were approved by the Institutional Review Board at the University of Massachusetts, Amherst. Written informed consent was obtained from participants.

AUTHOR CONTRIBUTIONS
Ahren B. Fitzroy: conceptualisation, methodology, software, formal analysis, investigation, data curation, writing-original draft and visualisation. Kyle Kainec: investigation, data curation and writing-review and editing. Rebecca M. C. Spencer: conceptualisation, supervision, project administration, funding acquisition and writing-review and editing.

PEER REVIEW
The peer review history for this article is available at https://publons.com/publon/10.1111/ejn.15468.

DATA AVAILABILITY STATEMENT
Processed data included in analyses are available for download (https://osf.io/wkhfj/). Raw data are not publicly shared because public release of raw data was not consented to by participants; for access to these data please contact the corresponding author to establish a data sharing agreement.

ORCID
Ahren B. Fitzroy https://orcid.org/0000-0003-1429-5308
Kyle A. Kainec https://orcid.org/0000-0001-9200-9923
Rebecca M. C. Spencer https://orcid.org/0000-0002-8674-2384

REFERENCES

Abe, O., Yamasue, H., Aoki, S., Suga, M., Yamada, H., Kasai, K., Masutani, Y., Kato, N., Kato, N., & Ohtomo, K. (2008). Aging in the CNS: Comparison of gray/white matter volume and diffusion tensor data. *Neurobiology of Aging*, 29(1), 102–116. https://doi.org/10.1016/j.neurobiolaging.2006.09.003

Albert, A. M., Ricanek, K., & Patterson, E. (2007). A review of the literature on the aging adult skull and face: Implications for forensic science research and applications. *Forensic Science International*, 172(1), 1–9. https://doi.org/10.1016/j.forsciint.2007.03.015

Alfonsi, V., D'Atri, A., Gorgoni, M., Scarpelli, S., Mangiaruga, A., Ferrara, M., & De Gennaro, L. (2019). Spatiotemporal dynamics of sleep spindle sources across NREM sleep cycles. *Frontiers in Neuroscience*, 13, 727. https://doi.org/10.3389/fnins.2019.00727

Aly, M., & Moscovitch, M. (2010). The effects of sleep on episodic memory in older and younger adults. *Memory*, 18(3), 327–334. https://doi.org/10.1080/09658211003601548

Andersson, J. L. R., Jenkinson, M., & Smith, S. (2007). Non-linear registration aka Spatial normalisation (FMRIB Technical Report TR07JA2). https://www.fmrib.ox.ac.uk/datasets/techrep/tr07ja2/tr07ja2.pdf

Andrillon, T., Nir, Y., Staba, R. J., Ferrarelli, F., Cirelli, C., Tononi, G., & Fried, I. (2011). Sleep spindles in humans: Insights from intracranial EEG and unit recordings. *Journal of Neuroscience*, 31(49), 17821–17834. https://doi.org/10.1523/JNEUROSCI.2604-11.2011

Baran, B., Mantua, J., & Spencer, R. M. C. (2016). Age-related changes in the sleep-dependent reorganization of declarative memories. *Journal of Cognitive Neuroscience*, 28(6), 792–802. https://doi.org/10.1162/jocn_a_00938

Baron, R. M., & Kenny, D. A. (1986). The moderator-mediator variable distinction in social psychological research: Conceptual, strategic, and statistical considerations. *Journal of Personality and Social Psychology*, 51(6), 1173–1182. https://doi.org/10.1037//0022-3514.51.6.1173

Beck, A. T., Steer, R. A., & Brown, G. K. (1996). Beck Depression Inventory-II. *San Antonio*, 78(2), 490–498.

Benjamini, Y., & Hochberg, Y. (1995). Controlling the false discovery rate: A practical and powerful approach to multiple testing. *Journal of the Royal Statistical Society*. Series B (Methodological), 57(1), 289–300. https://doi.org/10.1111/j.2517-6161.1995.tb02031.x

Bersagliere, A., Pascual-Marqui, R. D., Tarokh, L., & Achermann, P. (2018). Mapping slow waves by EEG topography and source localization: Effects of sleep deprivation. *Brain Topography*, 31(2), 257–269. https://doi.org/10.1007/s10548-017-0595-6

Borbély, A. A. (1982). A two process model of sleep regulation. *Human Neurobiology*, 1(3), 195–204.

Brandt, J., Spencer, M., & Folstein, M. (1988). The telephone interview for cognitive status. *Neuropsychiatry, Neuropsychology, & Behavioral Neurology*, 1(2), 111–117.

Buchmann, A., Ringli, M., Kurth, S., Schaerer, M., Geiger, A., Jenni, O. G., & Huber, R. (2011). EEG sleep slow-wave activity as a mirror of cortical maturation. *Cerebral Cortex*, 21(3), 607–615. https://doi.org/10.1093/cercor/bhq129

Buckner, R. L., Head, D., Parker, J., Fotenos, A. F., Marcus, D., Morris, J. C., & Snyder, A. Z. (2004). A unified approach for morphometric and functional data analysis in young, old, and demented adults using automated atlas-based head size normalization: Reliability and validation against manual measurement of total intracranial volume. *NeuroImage*, 23(2), 724–738. https://doi.org/10.1016/j.neuroimage.2004.06.018

Buysse, D. J., Reynolds, C. F., Monk, T. H., Berman, S. R., & Kupfer, D. J. (1989). The Pittsburgh sleep quality index: A new instrument for psychiatric practice and research. *Psychiatry Research*, 28(2), 193–213. https://doi.org/10.1016/0165-1781(89)90047-4

Campbell, I. G., & Feinberg, I. (2009). Longitudinal trajectories of non-rapid eye movement delta and theta EEG as indicators of adolescent brain maturation. *Proceedings of the National Academy of Sciences*, 106(13), 5177–5180. https://doi.org/10.1073/pnas.0812947106

Carrier, J., Land, S., Buysse, D. J., Kupfer, D. J., & Monk, T. H. (2001). The effects of age and gender on sleep EEG power spectral density in the middle years of life (ages 20-60 years old). *Psychophysiology*, 38(2), 232–242. https://doi.org/10.1111/1469-8986.3820232

Carrier, J., Viens, I., Poirier, G., Robillard, R., Lafortune, M., Vandewalle, G., Martin, N., Barakat, M., Paquet, J., & Filipini, D. (2011). Sleep slow wave changes during the middle years of life. *European Journal of Neuroscience*, 33(4), 758–766. https://doi.org/10.1111/j.1460-9568.2010.07543.x

Cherubini, A., Péran, P., Caltagirone, C., Sabatini, U., & Spalletta, G. (2009). Aging of subcortical nuclei: Microstructural, mineralization and atrophy modifications measured in vivo using MRI. *NeuroImage*, 48(1), 29–36. https://doi.org/10.1016/j.neuroimage.2009.06.035

Crowley, K., Trinder, J., Kim, Y., Carrington, M., & Colrain, I. M. (2002). The effects of normal aging on sleep spindle and K-complex production. *Clinical Neurophysiology*, 113(10), 1615–1622. https://doi.org/10.1016/S1388-2457(02)00237-7

Delorme, A., & Makeig, S. (2004). EEGLAB: An open source toolbox for analysis of single-trial EEG dynamics including independent component analysis. *Journal of Neuroscience Methods*, 134(1), 9–21. https://doi.org/10.1016/j.jneumeth.2003.10.009

Desikan, R. S., Ségonne, F., Fischl, B., Quinn, B. T., Dickerson, B. C., Blacker, D., Buckner, R. L., Dale, A. M., Maguire, R. P., Hyman, B. T., Albert, M. S., & Killiany, R. J. (2006). An automated labeling system for subdividing the human cerebral cortex on MRI scans into gyral based regions of interest. *NeuroImage*, 31(3), 968–980. https://doi.org/10.1016/j.neuroimage.2006.01.021

Diedrichsen, J., Balsters, J. H., Flavell, J., Cussans, E., & Ramnani, N. (2009). A probabilistic MR atlas of the human cerebellum. *NeuroImage*, 46(1), 39–46. https://doi.org/10.1016/j.neuroimage.2009.01.045

Diedrichsen, J., Maderwald, S., Küper, M., Thürling, M., Rabe, K., Gizewski, E. R., Ladd, M. E., & Timmann, D. (2011). Imaging the deep cerebellar nuclei: A probabilistic atlas and normalization procedure. *NeuroImage*, 54(3), 1786–1794. https://doi.org/10.1016/j.neuroimage.2010.10.035

Dijk, D.-J., Beersma, D. G. M., & Van den Hoofdakker, R. H. (1989). All night spectral analysis of EEG sleep in young adult

and middle-aged male subjects. *Neurobiology of Aging*, *10*(6), 677–682. https://doi.org/10.1016/0197-4580(89)90004-3

Dijk, D.-J., Brunner, D. P., Beersma, D. G. M., & Borbély, A. A. (1990). Electroencephalogram power density and slow wave sleep as a function of prior waking and circadian phase. *Sleep*, *13*(5), 430–440. https://doi.org/10.1093/sleep/13.5.430

Douaud, G., Smith, S., Jenkinson, M., Behrens, T., Johansen-Berg, H., Vickers, J., James, S., Voets, N., Watkins, K., Matthews, P. M., & James, A. (2007). Anatomically related grey and white matter abnormalities in adolescent-onset schizophrenia. *Brain*, *130*(9), 2375–2386. https://doi.org/10.1093/brain/awm184

Doyon, J., & Benali, H. (2005). Reorganization and plasticity in the adult brain during learning of motor skills. *Current Opinion in Neurobiology*, *15*(2), 161–167. https://doi.org/10.1016/j.conb.2005.03.004

Doyon, J., Gaudreau, D., Laforce, R. Jr., Castonguay, M., Bédard, P. J., Bédard, F., & Bouchard, J. P. (1997). Role of the striatum, cerebellum, and frontal lobes in the learning of a visuomotor sequence. *Brain and Cognition*, *34*(2), 218–245. https://doi.org/10.1006/brcg.1997.0899

Doyon, J., Penhune, V., & Ungerleider, L. G. (2003). Distinct contribution of the cortico-striatal and cortico-cerebellar systems to motor skill learning. *Neuropsychologia*, *41*(3), 252–262. https://doi.org/10.1016/S0028-3932(02)00158-6

Doyon, J., & Ungerleider, L. G. (2002). Functional anatomy of motor skill learning. In L. R. Squire & D. L. Schacter (Eds.), *Neuropsychology of Memory* (3rd ed. pp. 225–238). New York, NY: Guilford Press.

Dubé, J., Lafortune, M., Bedetti, C., Bouchard, M., Gagnon, J. F., Doyon, J., Evans, A. C., Lina, J.-M., & Carrier, J. (2015). Cortical thinning explains changes in sleep slow waves during adulthood. *Journal of Neuroscience*, *35*(20), 7795–7807. https://doi.org/10.1523/JNEUROSCI.3956-14.2015

Eichenlaub, J.-B., Jarosiewicz, B., Saab, J., Franco, B., Kelemen, J., Halgren, E., Hochberg, L. R., & Cash, S. S. (2020). Replay of learned neural firing sequences during rest in human motor cortex. *Cell Reports*, *31*(5), 107581. https://doi.org/10.1016/j.celrep.2020.107581

Eickhoff, S. B., Stephan, K. E., Mohlberg, H., Grefkes, C., Fink, G. R., Amunts, K., & Zilles, K. (2005). A new SPM toolbox for combining probabilistic cytoarchitectonic maps and functional imaging data. *NeuroImage*, *25*(4), 1325–1335. https://doi.org/10.1016/j.neuroimage.2004.12.034

Exner, C., Weniger, G., & Irle, E. (2001). Implicit and explicit memory after focal thalamic lesions. *Neurology*, *57*(11), 2054–2063. https://doi.org/10.1212/WNL.57.11.2054

Feinberg, I., de Bie, E., Davis, N. M., & Campbell, I. G. (2011). Topographic differences in the adolescent maturation of the slow wave EEG during NREM sleep. *Sleep*, *34*(3), 325–333. https://doi.org/10.1093/sleep/34.3.325

Finelli, L. A., Borbély, A. A., & Achermann, P. (2001). Functional topography of the human nonREM sleep electroencephalogram. *European Journal of Neuroscience*, *13*(12), 2282–2290. https://doi.org/10.1046/j.0953-816x.2001.01597.x

Fischl, B., Salat, D. H., Busa, E., Albert, M., Dieterich, M., Haselgrove, C., Van der Kouwe, A., Killiany, R., Kennedy, D., Klaveness, S., Montillo, A., Makris, N., Rosen, B., & Dale, A. M. (2002). Whole brain segmentation: Automated labeling of neuroanatomical structures in the human brain. *Neuron*, *33*(3), 341–355. https://doi.org/10.1016/s0896-6273(02)00569-x

Fitzroy, A. B., Kainec, K. A., Seo, J., & Spencer, R. M. C. (2021). Encoding and consolidation of motor sequence learning in young and older adults. *Neurobiology of Learning and Memory*, *185*, 107508. https://doi.org/10.1016/j.nlm.2021.107508

[Dataset] Fitzroy, A. B., Kainec, K. A., & Spencer, R. M. C. (2021). Aging-related changes in nap neuroscillatory activity are mediated and moderated by grey matter volume. Hosted on the Open Science Framework. https://osf.io/wkhfj/

Fogel, S., Albouy, G., Vien, C., Popovicci, R., King, B. R., Hoge, R., Jbabdi, S., Benali, H., Karni, A., Maquet, P., Carrier, J., & Doyon, J. (2014). fMRI and sleep correlates of the age-related impairment in motor memory consolidation. *Human Brain Mapping*, *35*(8), 3625–3645. https://doi.org/10.1002/hbm.22426

Fogel, S., Vien, C., Karni, A., Benali, H., Carrier, J., & Doyon, J. (2017). Sleep spindles: A physiological marker of age-related changes in gray matter in brain regions supporting motor skill memory consolidation. *Neurobiology of Aging*, *49*, 154–164. https://doi.org/10.1016/j.neurobiolaging.2016.10.009

Folstein, M. F., Folstein, S. E., & McHugh, P. R. (1975). Mini-mental state: A practical method for grading the cognitive state of patients for the clinician. *Journal of Psychiatric Research*, *12*(3), 189–198. https://doi.org/10.1016/0022-3956(75)90026-6

Frazier, J. A., Chiu, S., Breeze, J. L., Makris, N., Lange, N., Kennedy, D. N., Herbert, M. R., Bent, E. K., Koneru, V. K., Dieterich, M. E., Hodge, S. M., Rauch, S. L., Grant, P. E., Cohen, B. M., Seidman, L. J., Caviness, V. S., & Biederman, J. (2005). Structural brain magnetic resonance imaging of limbic and thalamic volumes in pediatric bipolar disorder. *The American Journal of Psychiatry*, *162*(7), 1256–1265. https://doi.org/10.1176/appi.ajp.162.7.1256

Freeman, W. J. (2004). Origin, structure, and role of background EEG activity. Part 1. Analytic amplitude. *Clinical Neurophysiology*, *115*(9), 2077–2088. https://doi.org/10.1016/j.clinph.2004.02.029

Gaudreau, H., Carrier, J., & Montplaisir, J. (2001). Age-related modifications of NREM sleep EEG: From childhood to middle age. *Journal of Sleep Research*, *10*(3), 165–172. https://doi.org/10.1046/j.1365-2869.2001.00252.x

Geyer, S. (2004). The microstructural border between the motor and the cognitive domain in the human cerebral cortex. *Advances in Anatomy, Embryology, and Cell Biology*, *174*(I–VIII), 1–89. https://doi.org/10.1007/978-3-642-18910-4

Geyer, S., Ledberg, A., Schleicher, A., Kinomura, S., Schormann, T., Bürgel, U., Klingberg, T., Larsson, J., Zilles, K., & Roland, P. E. (1996). Two different areas within the primary motor cortex of man. *Nature*, *382*(6594), 805–807. https://doi.org/10.1038/382805a0

Giedd, J. N., Blumenthal, J., Jeffries, N. O., Castellanos, F. X., Liu, H., Zijdenbos, A., Paus, T., Evans, A. C., & Rapoport, J. L. (1999). Brain development during childhood and adolescence: A longitudinal MRI study. *Nature Neuroscience*, *2*(10), 861–863. https://doi.org/10.1038/13158

Gogtay, N., Giedd, J. N., Lusk, L., Hayashi, K. M., Greenstein, D., Vaituzis, A. C., Nugent, T. F., Herman, D. H., Clasen, L. S., Toga, A. W., Rapoport, J. L., & Thompson, P. M. (2004). Dynamic mapping of human cortical development during

childhood through early adulthood. *Proceedings of the National Academy of Sciences of the United States of America*, 101(21), 8174–8179. https://doi.org/10.1073/pnas.0402680101

Goldstone, A., Willoughby, A. R., De Zambotti, M., Franzen, P. L., Kwon, D., Pohl, K. M., Pfefferbaum, A., Sullivan, E. V., Müller-Oehring, E. M., Prouty, D. E., Hasler, B. P., Clark, D. B., Colrain, I. M., & Baker, F. C. (2018). The mediating role of cortical thickness and gray matter volume on sleep slow-wave activity during adolescence. *Brain Structure and Function*, 223(2), 669–685. https://doi.org/10.1007/s00429-017-1509-9

Goncalves, S. I., De Munck, J. C., Verbunt, J. P. A., Bijma, F., Heethaar, R. M., & Lopes da Silva, F. (2003). In vivo measurement of the brain and skull resistivities using an EIT-based method and realistic models for the head. *IEEE Transactions on Biomedical Engineering*, 50(6), 754–767. https://doi.org/10.1109/TBME.2003.812164

Good, C. D., Johnsrude, I. S., Ashburner, J., Henson, R. N. A., Friston, K. J., & Frackowiak, R. S. J. (2001). A voxel-based morphometric study of ageing in 465 normal adult human brains. *NeuroImage*, 14(1), 21–36. https://doi.org/10.1006/nimg.2001.0786

Gunning-Dixon, F. M., Head, D., McQuain, J., Acker, J. D., & Raz, N. (1998). Differential aging of the human striatum: A prospective MR imaging study. *American Journal of Neuroradiology*, 19(8), 1501–1507.

He, M., Liu, F., Nummenmaa, A., Hämäläinen, M., Dickerson, B. C., & Purdon, P. L. (2021). Age-related EEG power reductions cannot be explained by changes of the conductivity distribution in the head due to brain atrophy. *Frontiers in Aging Neuroscience*, 13, 632310. https://doi.org/10.3389/fnagi.2021.632310

Helfrich, R. F., Mander, B. A., Jagust, W. J., Knight, R. T., & Walker, M. P. (2018). Old brains come uncoupled in sleep: Slow wave-spindle synchrony, brain atrophy, and forgetting. *Neuron*, 97(1), 221–230.e4. https://doi.org/10.1016/j.neuron.2017.11.020

Hoddes, E., Zarcone, V., Smythe, H., Phillips, R., & Dement, W. C. (1973). Quantification of sleepiness: A new approach. *Psychophysiology*, 10(4), 431–436. https://doi.org/10.1111/j.1469-8986.1973.tb00801.x

Horne, J. A., & Ostberg, O. (1976). A self-assessment questionnaire to determine morningness-eveningness in human circadian rhythms. *International Journal of Chronobiology*, 4(2), 97–110.

Huber, R., Felice Ghilardi, M., Massimini, M., & Tononi, G. (2004). Local sleep and learning. *Nature*, 430(6995), 78–81. https://doi.org/10.1038/nature02663

Hughes, J. (2020). reghelper: Helper functions for regression analysis. https://CRAN.R-project.org/package=reghelper

Iber, C. (2007). *The AASM Manual for the Scoring of Sleep and Associated Events: Rules, Terminology and Technical Specifications*. Westchester, IL: American Academy of Sleep Medicine.

Janacsek, K., Shattuck, K. F., Tagarelli, K. M., Lum, J. A. G., Turkeltaub, P. E., & Ullman, M. T. (2020). Sequence learning in the human brain: A functional neuroanatomical meta-analysis of serial reaction time studies. *NeuroImage*, 207, 116387. https://doi.org/10.1016/j.neuroimage.2019.116387

Johns, M. W. (1991). A new method for measuring daytime sleepiness: The Epworth sleepiness scale. *Sleep*, 14(6), 540–545. https://doi.org/10.1093/sleep/14.6.540

Jones, B. J., & Spencer, R. M. C. (2020). Role of napping for learning across the lifespan. *Current Sleep Medicine Reports*, 6, 290–297. https://doi.org/10.1007/s40675-020-00193-9

King, B. R., Saucier, P., Albouy, G., Fogel, S. M., Rumpf, J.-J., Klann, J., Buccino, G., Binkofski, F., Classen, J., Karni, A., & Doyon, J. (2017). Cerebral activation during initial motor learning forecasts subsequent sleep-facilitated memory consolidation in older adults. *Cerebral Cortex*, 27(2), 1588–1601. https://doi.org/10.1093/cercor/bhv347

Kurth, S., Ringli, M., Geiger, A., LeBourgeois, M., Jenni, O. G., & Huber, R. (2010). Mapping of cortical activity in the first two decades of life: A high-density sleep electroencephalogram study. *Journal of Neuroscience*, 30(40), 13211–13219. https://doi.org/10.1523/JNEUROSCI.2532-10.2010

Landolt, H.-P., & Borbély, A. A. (2001). Age-dependent changes in sleep EEG topography. *Clinical Neurophysiology*, 112(2), 369–377. https://doi.org/10.1016/S1388-2457(00)00542-3

Landolt, H.-P., Dijk, D.-J., Achermann, P., & Borbély, A. A. (1996). Effect of age on the sleep EEG: Slow-wave activity and spindle frequency activity in young and middle-aged men. *Brain Research*, 738(2), 205–212. https://doi.org/10.1016/S0006-8993(96)00770-6

Latreille, V., Gaubert, M., Dubé, J., Lina, J.-M., Gagnon, J.-F., & Carrier, J. (2019). Age-related cortical signatures of human sleep electroencephalography. *Neurobiology of Aging*, 76, 106–114. https://doi.org/10.1016/j.neurobiolaging.2018.12.012

Lopez-Calderon, J., & Luck, S. J. (2014). ERPLAB: An open-source toolbox for the analysis of event-related potentials. *Frontiers in Human Neuroscience*, 8, 213. https://doi.org/10.3389/fnhum.2014.00213

Lynnerup, N. (2001). Cranial thickness in relation to age, sex and general body build in a Danish forensic sample. *Forensic Science International*, 117(1), 45–51. https://doi.org/10.1016/S0379-0738(00)00447-3

MacKinnon, D. P., Fairchild, A. J., & Fritz, M. S. (2007). Mediation analysis. *Annual Review of Psychology*, 58, 593–614. https://doi.org/10.1146/annurev.psych.58.110405.085542

Mander, B. A., Rao, V., Lu, B., Saletin, J. M., Ancoli-Israel, S., Jagust, W. J., & Walker, M. P. (2014). Impaired prefrontal sleep spindle regulation of hippocampal-dependent learning in older adults. *Cerebral Cortex*, 24(12), 3301–3309. https://doi.org/10.1093/cercor/bht188

Mander, B. A., Rao, V., Lu, B., Saletin, J. M., Lindquist, J. R., Ancoli-Israel, S., Jagust, W., & Walker, M. P. (2013). Prefrontal atrophy, disrupted NREM slow waves and impaired hippocampal-dependent memory in aging. *Nature Neuroscience*, 16(3), 357–364. https://doi.org/10.1038/nn.3324

Mander, B. A., Winer, J. R., & Walker, M. P. (2017). Sleep and human aging. *Neuron*, 94(1), 19–36. https://doi.org/10.1016/j.neuron.2017.02.004

Mantua, J., & Spencer, R. M. C. (2017). Exploring the nap paradox: Are mid-day sleep bouts a friend or foe? *Sleep Medicine*, 37, 88–97. https://doi.org/10.1016/j.sleep.2017.01.019

Maris, E., & Oostenveld, R. (2007). Nonparametric statistical testing of EEG- and MEG-data. *Journal of Neuroscience Methods*,

164(1), 177–190. https://doi.org/10.1016/j.jneumeth.2007.03.024

Martin, N., Lafortune, M., Godbout, J., Barakat, M., Robillard, R., Poirier, G., Bastien, C., & Carrier, J. (2013). Topography of age-related changes in sleep spindles. *Neurobiology of Aging*, *34*(2), 468–476. https://doi.org/10.1016/j.neurobiolaging.2012.05.020

McCann, H., Pisano, G., & Beltrachini, L. (2019). Variation in reported human head tissue electrical conductivity values. *Brain Topography*, *32*(5), 825–858. https://doi.org/10.1007/s10548-019-00710-2

McClain, I. J., Lustenberger, C., Achermann, P., Lassonde, J. M., Kurth, S., & LeBourgeois, M. K. (2016). Developmental changes in sleep spindle characteristics and sigma power across early childhood. *Neural Plasticity*, *2016*, 3670951. https://doi.org/10.1155/2016/3670951

Mitchell, A. J. (2009). A meta-analysis of the accuracy of the mini-mental state examination in the detection of dementia and mild cognitive impairment. *Journal of Psychiatric Research*, *43*(4), 411–431. https://doi.org/10.1016/j.jpsychires.2008.04.014

Münch, M., Knoblauch, V., Blatter, K., Schröder, C., Schnitzler, C., Kräuchi, K., Wirz-Justice, A., & Cajochen, C. (2004). The frontal predominance in human EEG delta activity after sleep loss decreases with age. *European Journal of Neuroscience*, *20*(5), 1402–1410. https://doi.org/10.1111/j.1460-9568.2004.03580.x

Münch, M., Knoblauch, V., Blatter, K., Wirz-Justice, A., & Cajochen, C. (2007). Is homeostatic sleep regulation under low sleep pressure modified by age? *Sleep: Journal of Sleep and Sleep Disorders Research*, *30*(6), 781–792. https://doi.org/10.1093/sleep/30.6.781

Münch, M., Silva, E. J., Ronda, J. M., Czeisler, C. A., & Duffy, J. F. (2010). EEG sleep spectra in older adults across all circadian phases during NREM sleep. *Sleep*, *33*(3), 389–401. https://doi.org/10.1093/sleep/33.3.389

Nicolas, A., Petit, D., Rompré, S., & Montplaisir, J. (2001). Sleep spindle characteristics in healthy subjects of different age groups. *Clinical Neurophysiology*, *112*(3), 521–527. https://doi.org/10.1016/S1388-2457(00)00556-3

Nir, Y., Staba, R. J., Andrillon, T., Vyazovskiy, V. V., Cirelli, C., Fried, I., & Tononi, G. (2011). Regional slow waves and spindles in human sleep. *Neuron*, *70*(1), 153–169. https://doi.org/10.1016/j.neuron.2011.02.043

Nishida, M., & Walker, M. P. (2007). Daytime naps, motor memory consolidation and regionally specific sleep spindles. *PLoS ONE*, *2*(4), e341. https://doi.org/10.1371/journal.pone.0000341

Nitsche, M. A., Schauenburg, A., Lang, N., Liebetanz, D., Exner, C., Paulus, W., & Tergau, F. (2003). Facilitation of implicit motor learning by weak transcranial direct current stimulation of the primary motor cortex in the human. *Journal of Cognitive Neuroscience*, *15*(4), 619–626. https://doi.org/10.1162/089892903321662994

Nobili, L., De Gennaro, L., Proserpio, P., Moroni, F., Sarasso, S., Pigorini, A., De Carli, F., & Ferrara, M. (2012). Local aspects of sleep: Observations from intracerebral recordings in humans. *Progress in Brain Research*, *199*, 219–232. https://doi.org/10.1016/B978-0-444-59427-3.00013-7

Nobili, L., Ferrara, M., Moroni, F., De Gennaro, L., Russo, G. L., Campus, C., Cardinale, F., & De Carli, F. (2011). Dissociated wake-like and sleep-like electro-cortical activity during sleep. *NeuroImage*, *58*(2), 612–619. https://doi.org/10.1016/j.neuroimage.2011.06.032

Oostenveld, R., Fries, P., Maris, E., & Schoffelen, J.-M. (2011). FieldTrip: Open source software for advanced analysis of MEG, EEG, and invasive electrophysiological data. *Computational Intelligence and Neuroscience*, *2011*, 1–9. https://doi.org/10.1155/2011/156869

Peters, K. R., Ray, L. B., Fogel, S., Smith, V., & Smith, C. T. (2014). Age differences in the variability and distribution of sleep spindle and rapid eye movement densities. *PLoS ONE*, *9*(3), e91047. https://doi.org/10.1371/journal.pone.0091047

R Core Team. (2020). R: A language and environment for statistical computing (3.6.3) [Computer software]. R Foundation for Statistical Computing. https://www.R-project.org/

Rasch, B., & Born, J. (2013). About sleep's role in memory. *Physiological Reviews*, *93*(2), 681–766. https://doi.org/10.1152/physrev.00032.2012

Raz, N., Rodrigue, K. M., Kennedy, K. M., Head, D., Gunning-Dixon, F., & Acker, J. D. (2003). Differential aging of the human striatum: Longitudinal evidence. *American Journal of Neuroradiology*, *24*(9), 1849–1856.

Robillard, R., Massicotte-Marquez, J., Kawinska, A., Paquet, J., Frenette, S., & Carrier, J. (2010). Topography of homeostatic sleep pressure dissipation across the night in young and middle-aged men and women. *Journal of Sleep Research*, *19*(3), 455–465. https://doi.org/10.1111/j.1365-2869.2010.00820.x

RStudio Team. (2018). RStudio: Integrated development environment for R (1.2.1335) [computer software]. RStudio, Inc. http://www.rstudio.com/

Saletin, J. M., & Greer, S. (2015). Hume software package (previously sleepSMG): Open-source MATLAB user interface for scoring sleep [MATLAB]. https://github.com/jsaletin/hume

Saletin, J. M., Van der Helm, E., & Walker, M. P. (2013). Structural brain correlates of human sleep oscillations. *NeuroImage*, *83*, 658–668. https://doi.org/10.1016/j.neuroimage.2013.06.021

Salimi-Khorshidi, G., Smith, S. M., & Nichols, T. E. (2011). Adjusting the effect of nonstationarity in cluster-based and TFCE inference. *NeuroImage*, *54*(3), 2006–2019. https://doi.org/10.1016/j.neuroimage.2010.09.088

Scholle, S., Zwacka, G., & Scholle, H. C. (2007). Sleep spindle evolution from infancy to adolescence. *Clinical Neurophysiology*, *118*(7), 1525–1531. https://doi.org/10.1016/j.clinph.2007.03.007

Schwarz, J. F. A., Åkerstedt, T., Lindberg, E., Gruber, G., Fischer, H., & Theorell-Haglöw, J. (2017). Age affects sleep microstructure more than sleep macrostructure. *Journal of Sleep Research*, *26*(3), 277–287. https://doi.org/10.1111/jsr.12478

Shaw, P., Kabani, N. J., Lerch, J. P., Eckstrand, K., Lenroot, R., Gogtay, N., Greenstein, D., Clasen, L., Evans, A., Rapoport, J. L., Giedd, J. N., & Wise, S. P. (2008). Neurodevelopmental trajectories of the human cerebral cortex. *Journal of Neuroscience*, *28*(14), 3586–3594. https://doi.org/10.1523/JNEUROSCI.5309-07.2008

Shinomiya, S., Nagata, K., Takahashi, K., & Masumura, T. (1999). Development of sleep spindles in young children and

adolescents. *Clinical Electroencephalography*, *30*(2), 39–43. https://doi.org/10.1177/155005949903000203

Siclari, F., & Tononi, G. (2017). Local aspects of sleep and wakefulness. *Current Opinion in Neurobiology*, *44*, 222–227. https://doi.org/10.1016/j.conb.2017.05.008

Smith, S. M., Jenkinson, M., Woolrich, M. W., Beckmann, C. F., Behrens, T. E. J., Johansen-Berg, H., Bannister, P. R., De Luca, M., Drobnjak, I., Flitney, D. E., Niazy, R. K., Saunders, J., Vickers, J., Zhang, Y., De Stefano, N., Brady, J. M., & Matthews, P. M. (2004). Advances in functional and structural MR image analysis and implementation as FSL. *NeuroImage*, *23*, S208–S219. https://doi.org/10.1016/j.neuroimage.2004.07.051

Soetens, E., Melis, A., & Notebaert, W. (2004). Sequence learning and sequential effects. *Psychological Research*, *69*(1), 124–137. https://doi.org/10.1007/s00426-003-0163-4

Sonni, A., & Spencer, R. M. C. (2015). Sleep protects memories from interference in older adults. *Neurobiology of Aging*, *36*(7), 2272–2281. https://doi.org/10.1016/j.neurobiolaging.2015.03.010

Spencer, R. M. C., Gouw, A. M., & Ivry, R. B. (2007). Age-related decline of sleep-dependent consolidation. *Learning & Memory*, *14*(7), 480–484. https://doi.org/10.1101/lm.569407

Sprecher, K. E., Riedner, B. A., Smith, R. F., Tononi, G., Davidson, R. J., & Benca, R. M. (2016). High resolution topography of age-related changes in non-rapid eye movement sleep electroencephalography. *PLoS ONE*, *11*(2), e0149770. https://doi.org/10.1371/journal.pone.0149770

Taki, Y., Goto, R., Evans, A., Zijdenbos, A., Neelin, P., Lerch, J., Sato, K., Ono, S., Kinomura, S., Nakagawa, M., Sugiura, M., Watanabe, J., Kawashima, R., & Fukuda, H. (2004). Voxel-based morphometry of human brain with age and cerebrovascular risk factors. *Neurobiology of Aging*, *25*(4), 455–463. https://doi.org/10.1016/j.neurobiolaging.2003.09.002

Tanguay, P. E., Ornitz, E. M., Kaplan, A., & Bozzo, E. S. (1975). Evolution of sleep spindles in childhood. *Electroencephalography and Clinical Neurophysiology*, *38*(2), 175–181. https://doi.org/10.1016/0013-4694(75)90227-8

Terpening, Z., Naismith, S., Melehan, K., Gittins, C., Bolitho, S., & Lewis, S. J. G. (2013). The contribution of nocturnal sleep to the consolidation of motor skill learning in healthy ageing and Parkinson's disease. *Journal of Sleep Research*, *22*(4), 398–405. https://doi.org/10.1111/jsr.12028

Tingley, D., Yamamoto, T., Hirose, K., Keele, L., & Imai, K. (2014). Mediation: R package for causal mediation analysis. *Journal of Statistical Software*, *59*(5). https://doi.org/10.18637/jss.v059.i05

Vyazovskiy, V. V., & Tobler, I. (2005). Regional differences in NREM sleep slow-wave activity in mice with congenital callosal dysgenesis. *Journal of Sleep Research*, *14*(3), 299–304. https://doi.org/10.1111/j.1365-2869.2005.00456.x

Wendel, K., Väisänen, J., Seemann, G., Hyttinen, J., & Malmivuo, J. (2010). The influence of age and skull conductivity on surface and subdermal bipolar EEG leads. *Computational Intelligence and Neuroscience*, *2010*, e397272. https://doi.org/10.1155/2010/397272

Werth, E., Achermann, P., & Borbély, A. (1997). Fronto-occipital EEG power gradients in human sleep. *Journal of Sleep Research*, *6*(2), 102–112. https://doi.org/10.1046/j.1365-2869.1997.d01-36.x

Wilson, J. K., Baran, B., Pace-Schott, E. F., Ivry, R. B., & Spencer, R. M. C. (2012). Sleep modulates word-pair learning but not motor sequence learning in healthy older adults. *Neurobiology of Aging*, *33*(5), 991–1000. https://doi.org/10.1016/j.neurobiolaging.2011.06.029

Wilson, M. A., & McNaughton, B. L. (1994). Reactivation of hippocampal ensemble memories during sleep. *Science*, *265*(5172), 676–679. https://doi.org/10.1126/science.8036517

Winkler, A. M., Ridgway, G. R., Webster, M. A., Smith, S. M., & Nichols, T. E. (2014). Permutation inference for the general linear model. *NeuroImage*, *92*, 381–397. https://doi.org/10.1016/j.neuroimage.2014.01.060

SUPPORTING INFORMATION

Additional supporting information may be found in the online version of the article at the publisher's website.